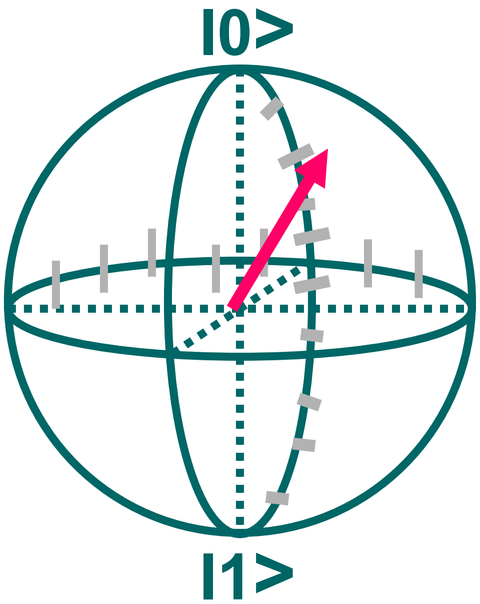

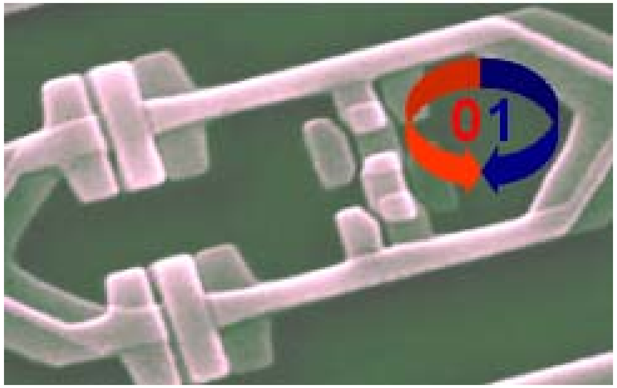

SUPERCONDUCTING QUANTUM BITS

Hans Mooij

Summer School on
Condensed Matter Theory
Windsor, August 18, 2004

quantum computer

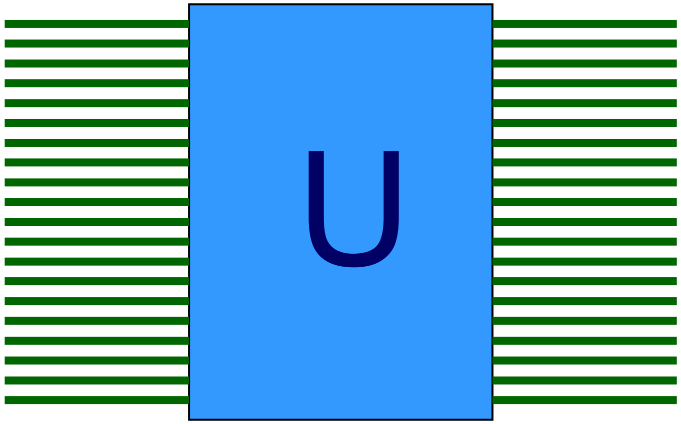

input - unitary transformations - output

N qubits, 2^N states

quantum algorithms
  factorization (Shor)
  searching (Grover)

error correction

quantum bits
  states I0>, I1>
  $\Psi = \alpha|0\rangle + \beta|1\rangle$

initialization
controlled operations
interaction
large number
individual readout

non-trivial two-bit gates
  controlled-not, swap

quantum bit: two level quantum system

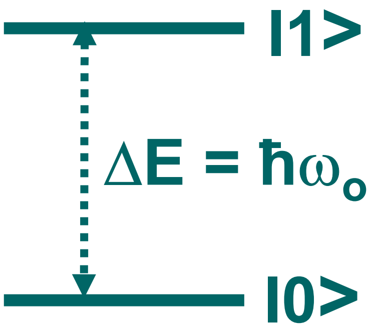

Ψ = α I0> + β I1>

IαI^2 + IβI^2 = 1

α = cos θ β = e$^{i\phi}$ sin θ

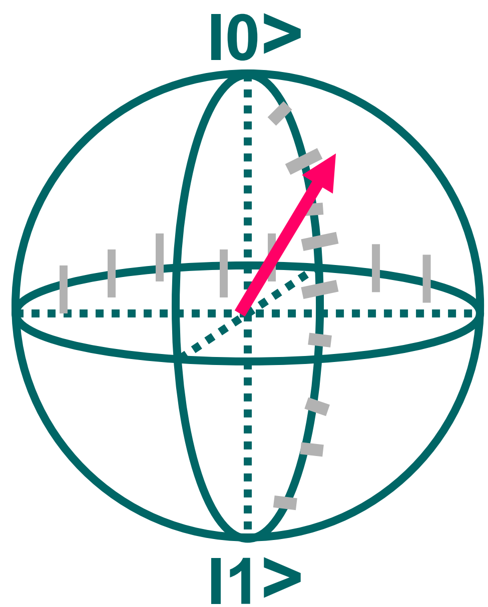

latitude:
angle θ
content I0> and I1>
measured in readout

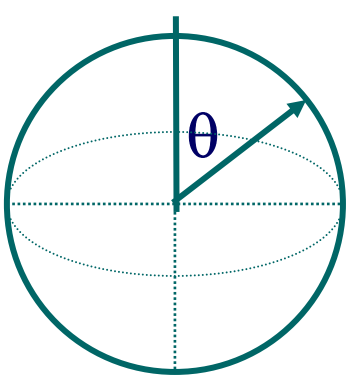

longitude:
phase ϕ
irrelevant in readout
dϕ/dt = ΔE/ħ

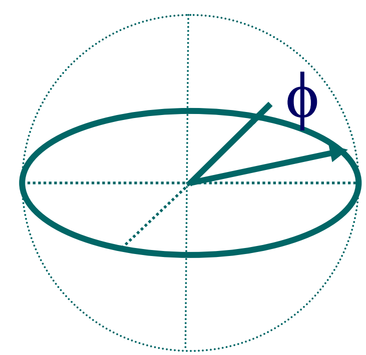

quantum manipulations

resonant electromagnetic wave $\nu = \Delta E/h$

Rabi oscillation

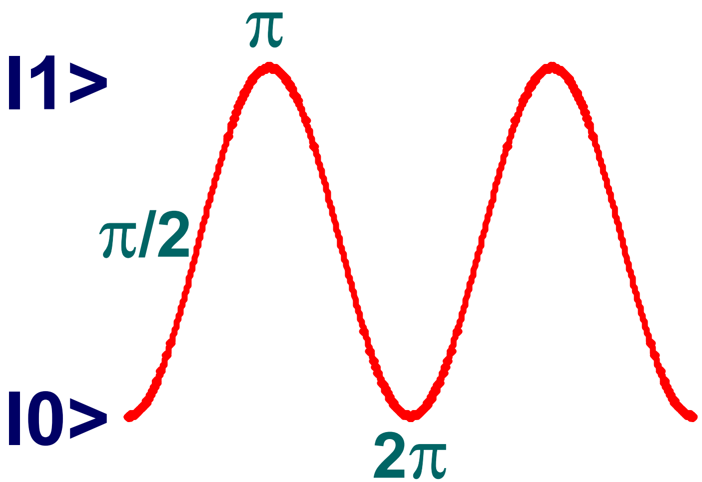

$\Psi = \alpha|0\rangle + \beta|1\rangle$

$\alpha(t) = \cos(\theta_o + \omega_R t)$

$\beta(t) = \sin(\theta_o + \omega_R t)$

length of microwave pulse determines final state

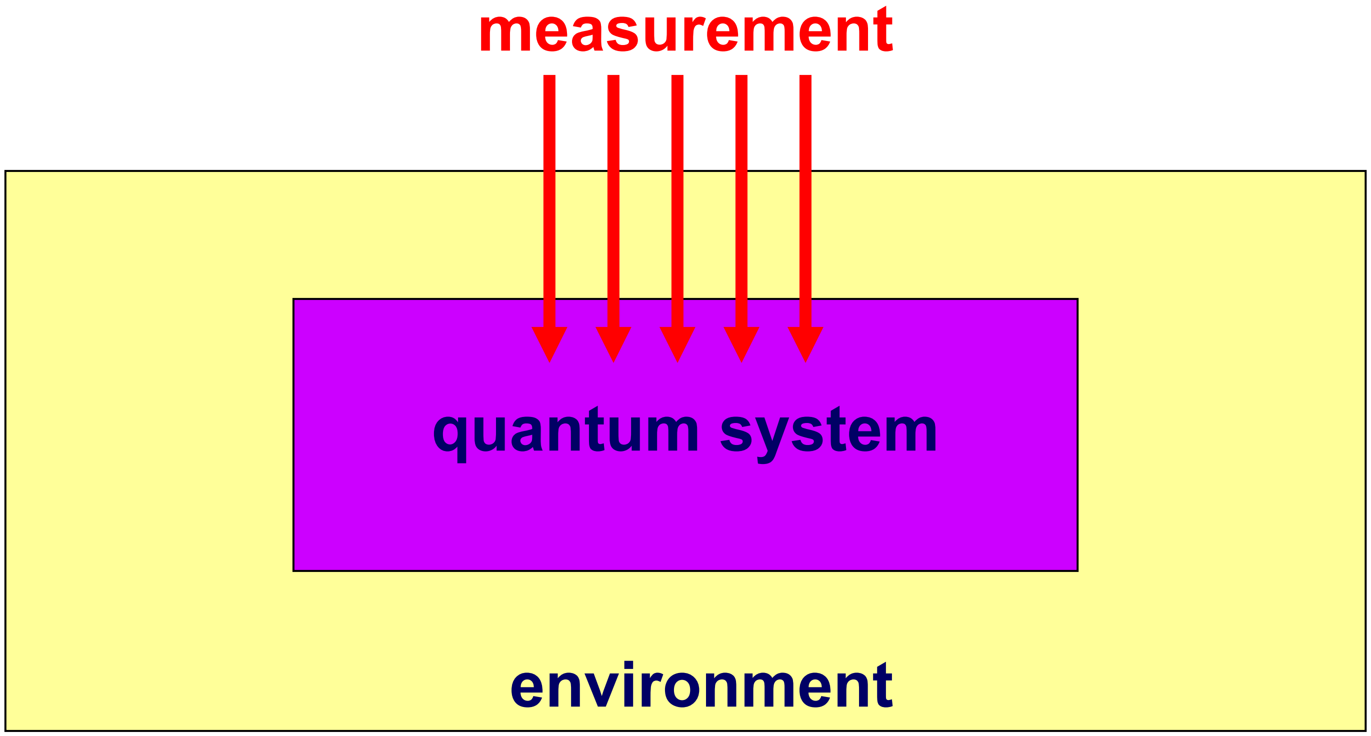
measurement
quantum system
environment

well-established quantum technologies

- **nuclear magnetic resonance**
- **photons**
- **ions / atoms**

basic manipulations well-controlled
in present form not scalable

NMR

10^{18} identical molecules in liquid

each molecule has N identifiable spins

10^{18} parallel N-qubit computers

ensemble-properties represent qubits

readout: measurement of spin magnetic moments

nuclear spins

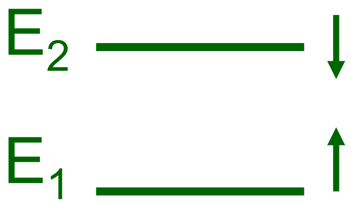

E_2-E_1 proportional to magnetic field strength

weak interaction between the spins in the same molecule

no interaction between molecules

Deutsch-Jozsa

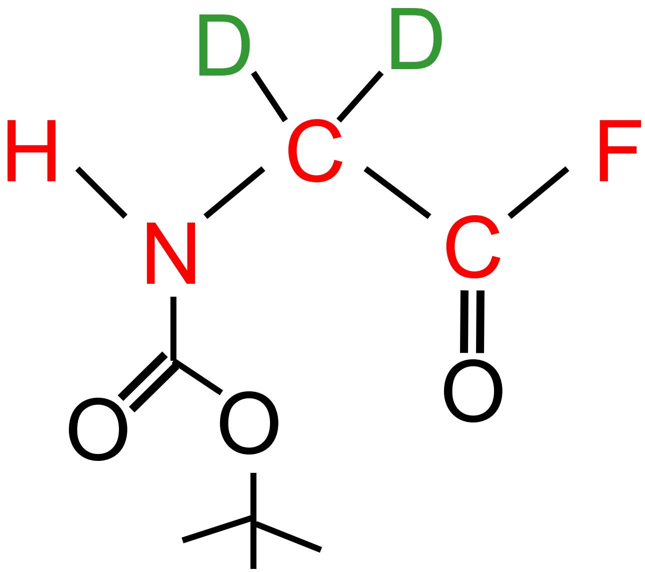

7-spin coherence

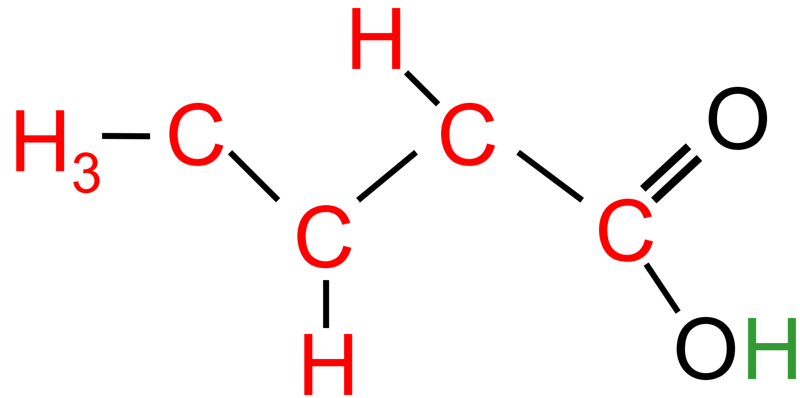

Order-finding

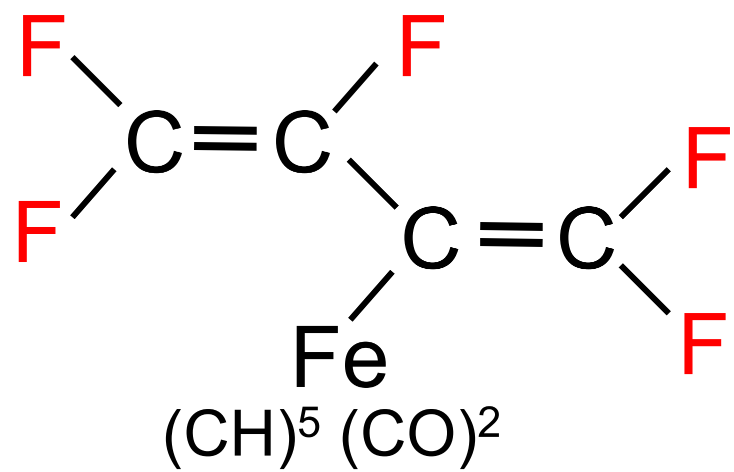

factoring 15 with nuclear spins

Vandersypen et al., *Nature* **414**, 883 (2001)

15 ≈ 3 x 5

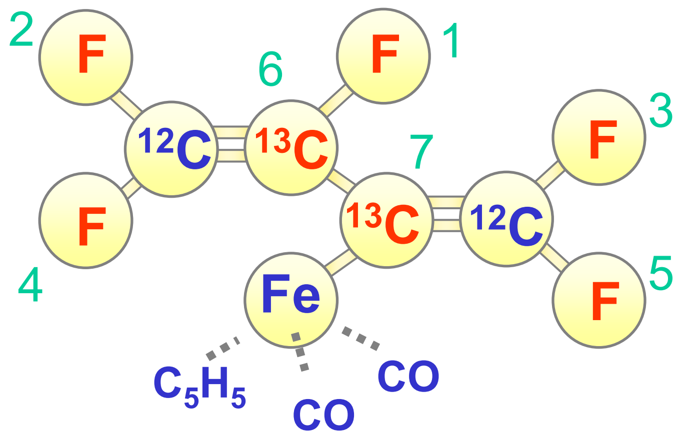

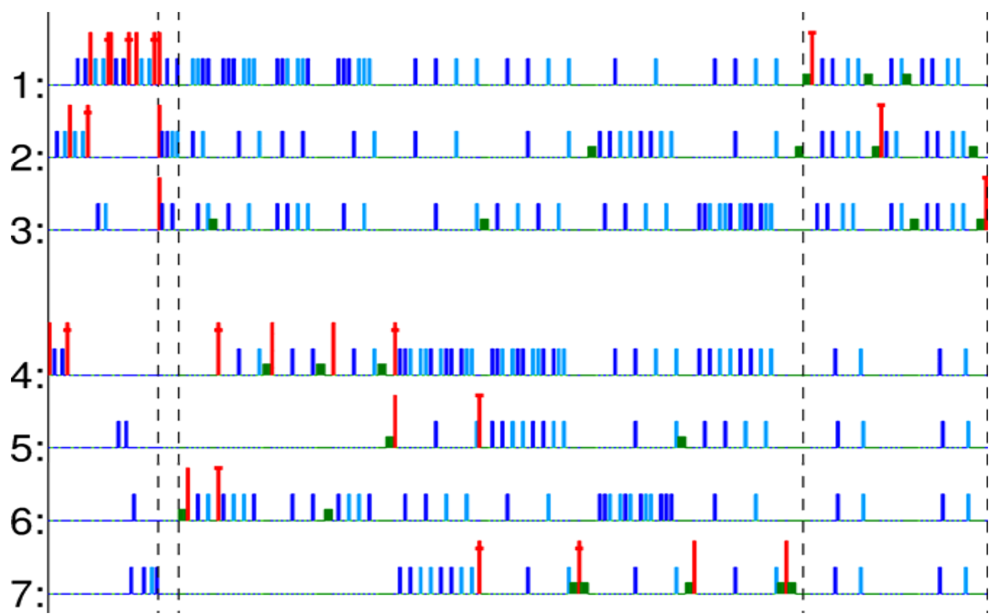

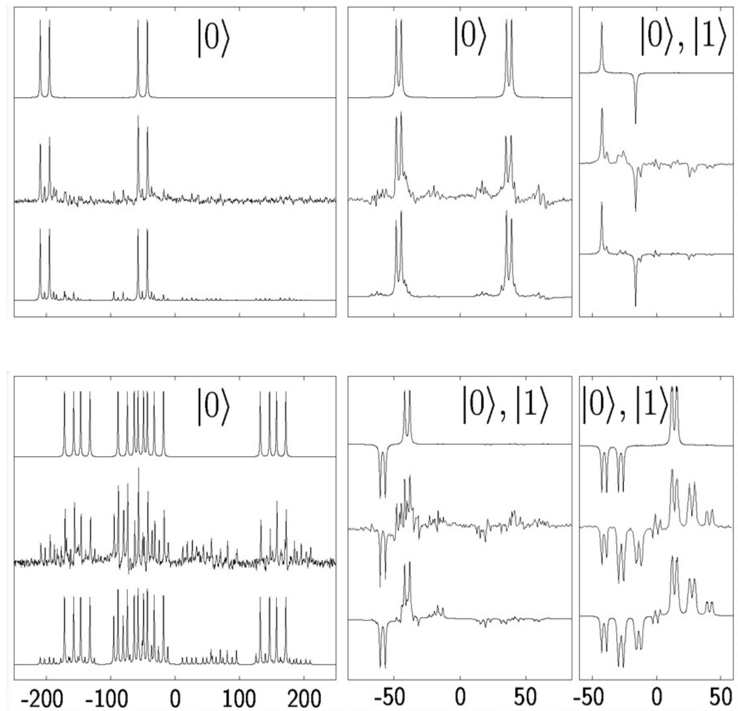

photons

'free' single photons
- beam splitters
- polarizers
- non-linear Kerr cells
- single photon detectors

photons in a cavity
- interaction through an atom

ions in an ion trap

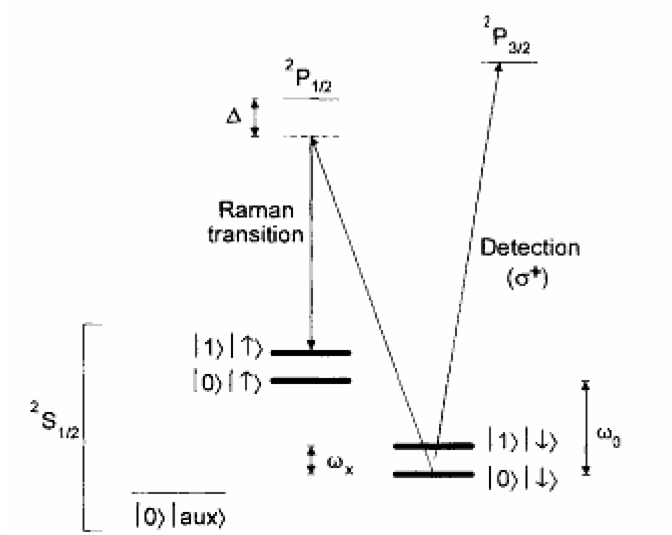

c. monroe et al. PRL **75** 4714 1995

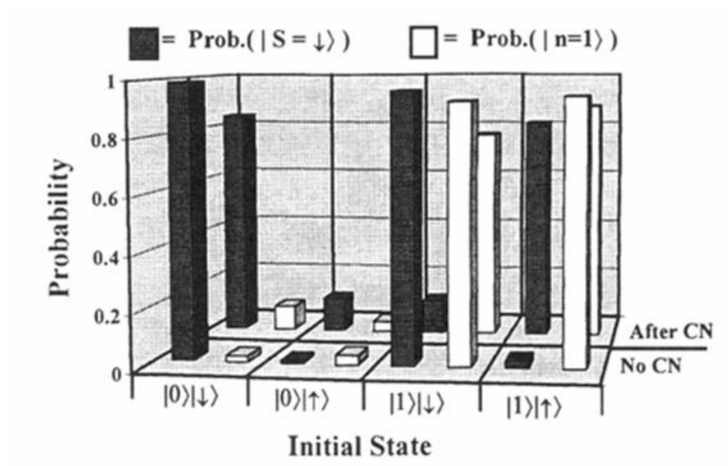

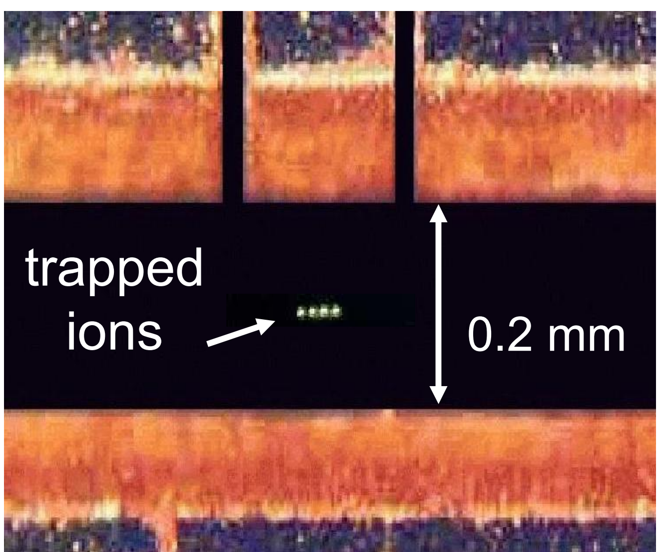

Courtesy D. Wineland, NIST

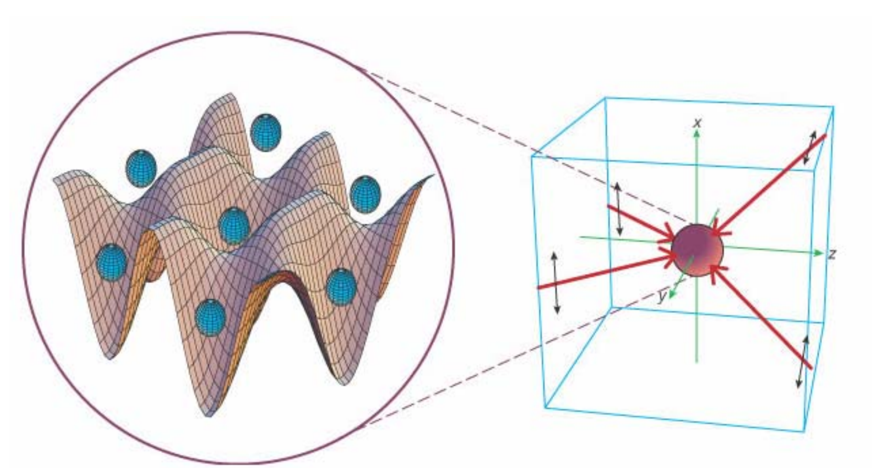

new scalable quantum technologies

- ion traps with micro-control electrodes 'atom chip'
- superconducting systems
- single spins in semiconductors
- x x x x

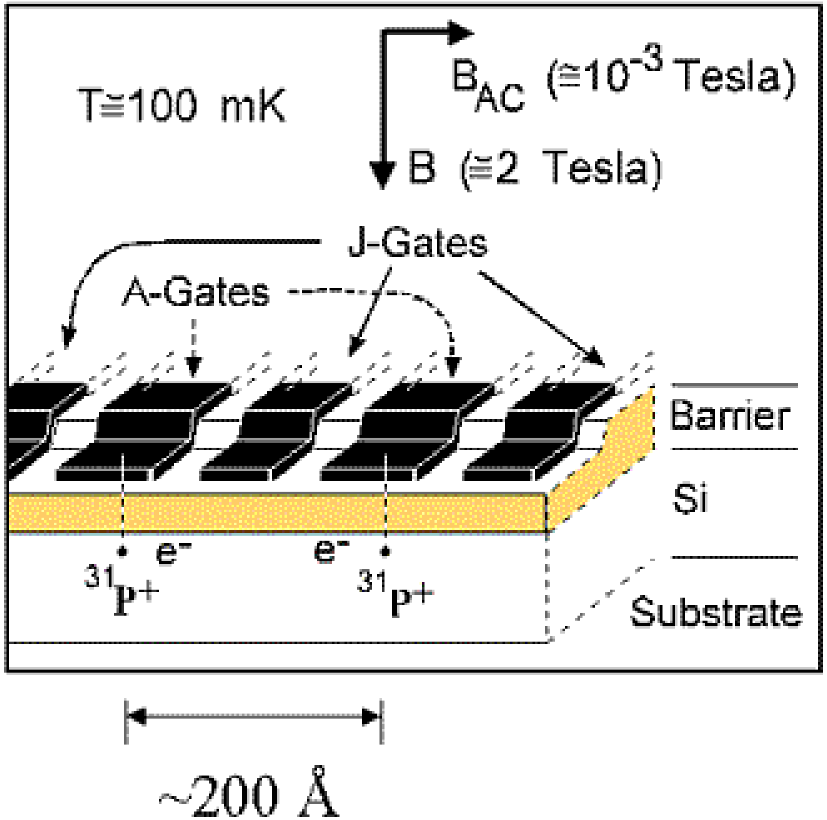

"A Silicon-based nuclear spin quantum computer"

B. E. Kane, *Nature*, May 14, 1998

also, quant-ph/0003031

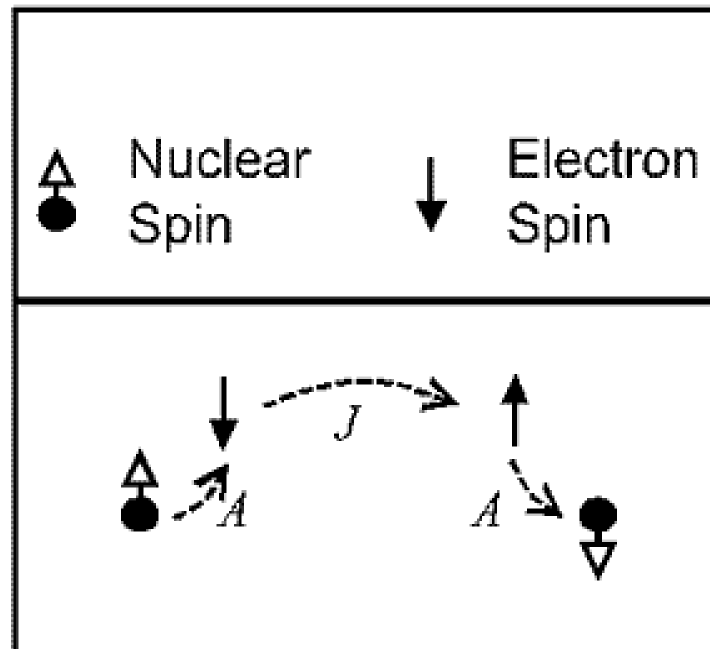

single spins in a semiconductor

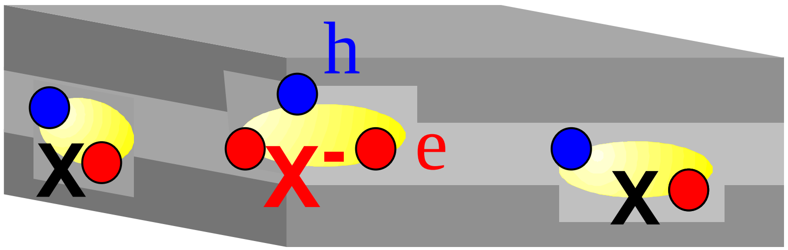

Gammon et al
Imamoglu et al, PRL 1999

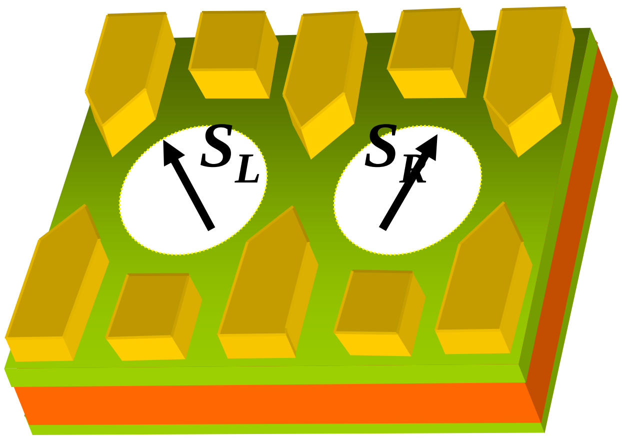

Loss & DiVincenzo, PRA 1998

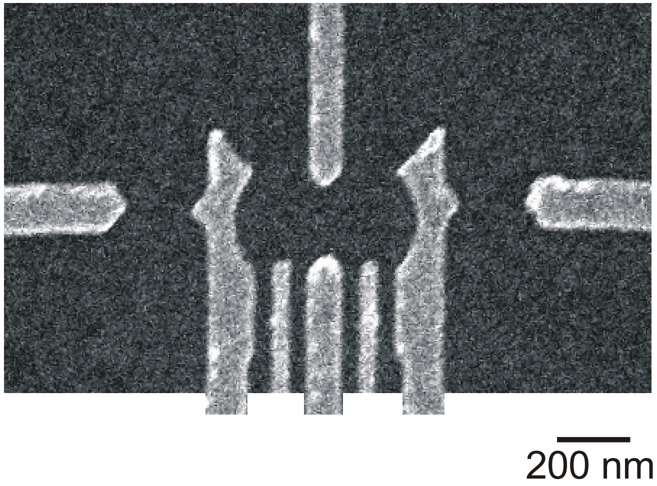

mesoscopic Josephson junction circuits

Josephson coupling energy

$$U_J = E_J\,(1 - \cos\phi)$$

$$E_J = 2\Delta\,(h/e^2)\,/\,(8R_n)$$

Coulomb charging energy

$$U_C = E_C\,4n^2$$

$$E_C = e^2 / 2C$$

$E_J/E_C >> 1$
phase excitations
fluxons

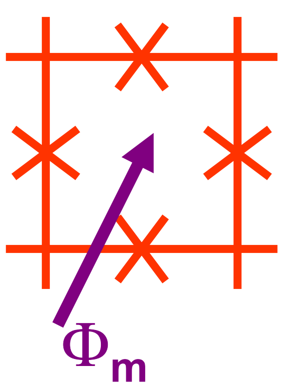

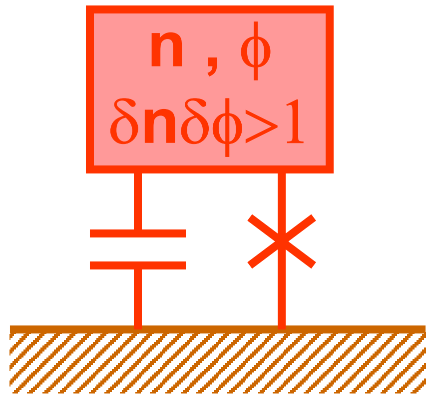

$E_C/E_J >> 1$
charge excitations

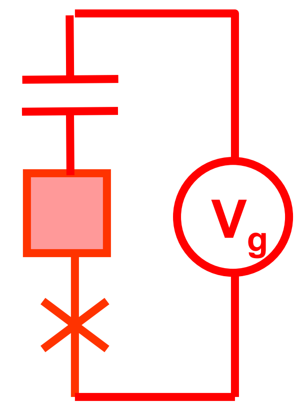

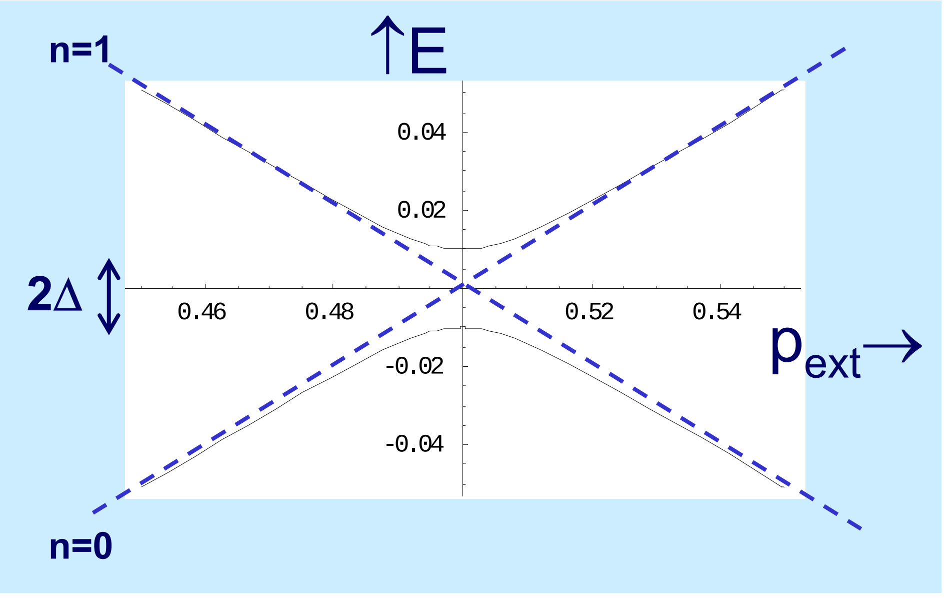

charge qubit

$p_{ext} = V_g C_g / 2e$

$\Delta = E_J$

n : Cooper pairs

flux qubit

$p_{ext} = \Phi / \Phi_o$

$\Delta : \exp\{ -(E_J/E_c)^{1/2} \}$

n : fluxons

Nakamura, Pashkin, Tsai

Nature 398, 786 (1999)

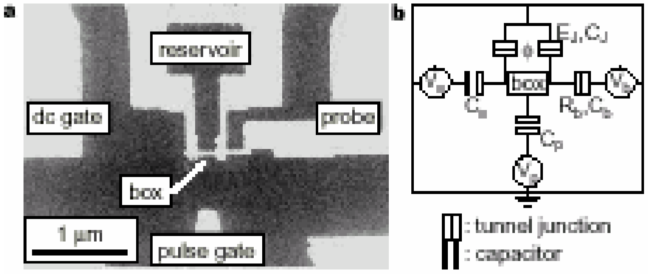

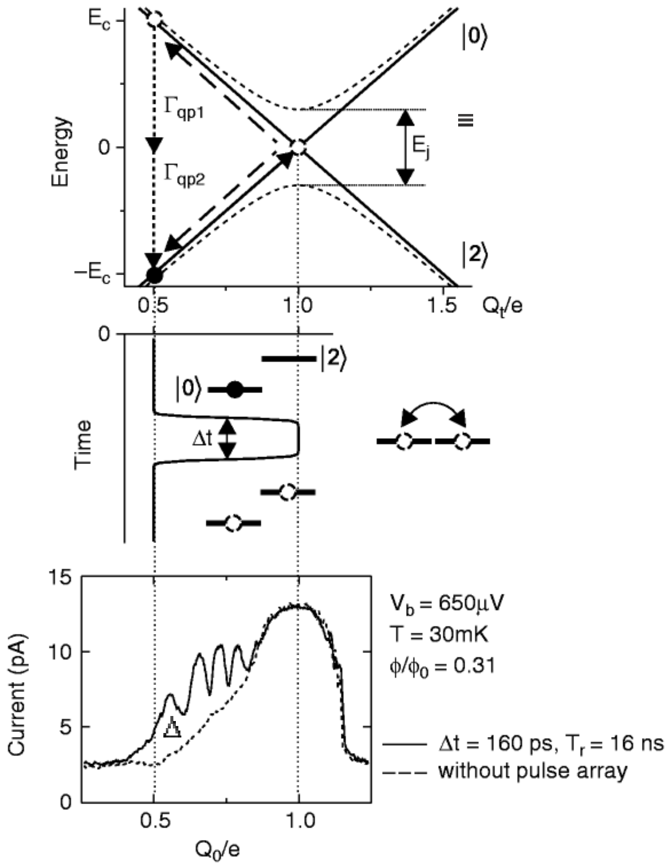

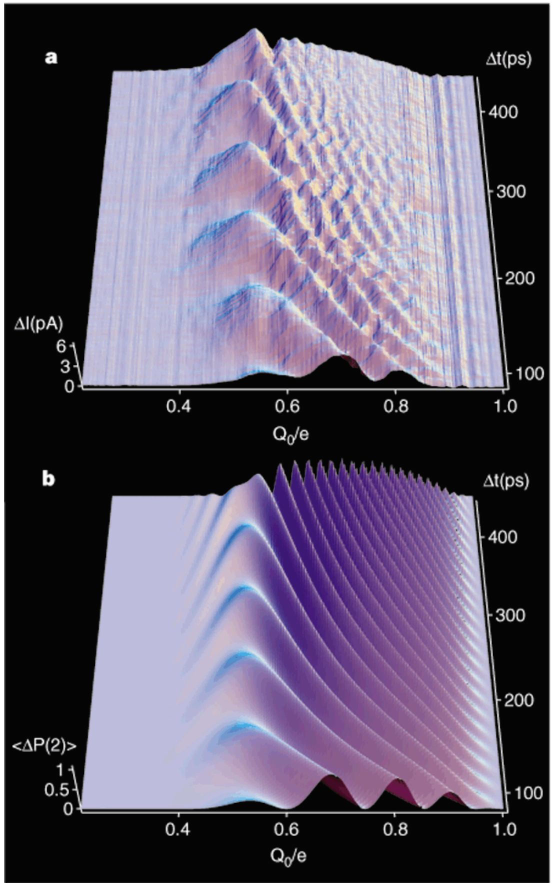

Yamamoto, Pashkin, Astaflev, Nakamura, Tsai
Nature 425, 941 (2003)

CNOT

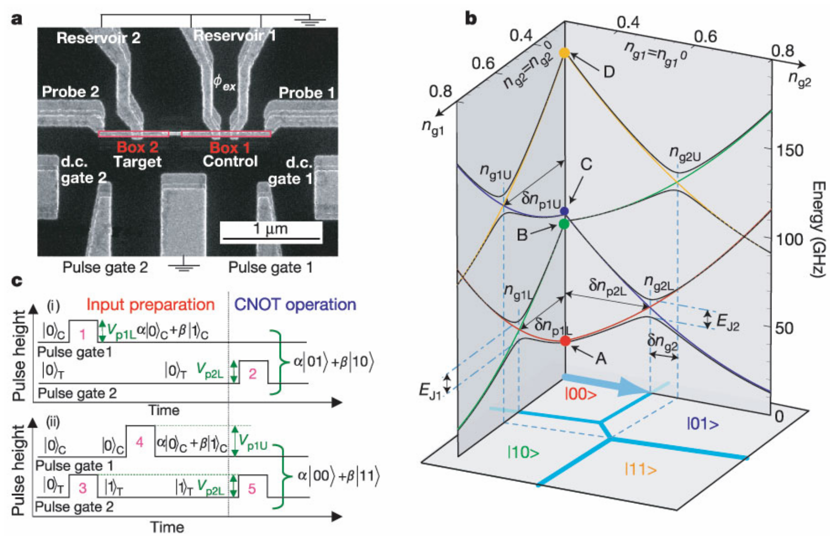

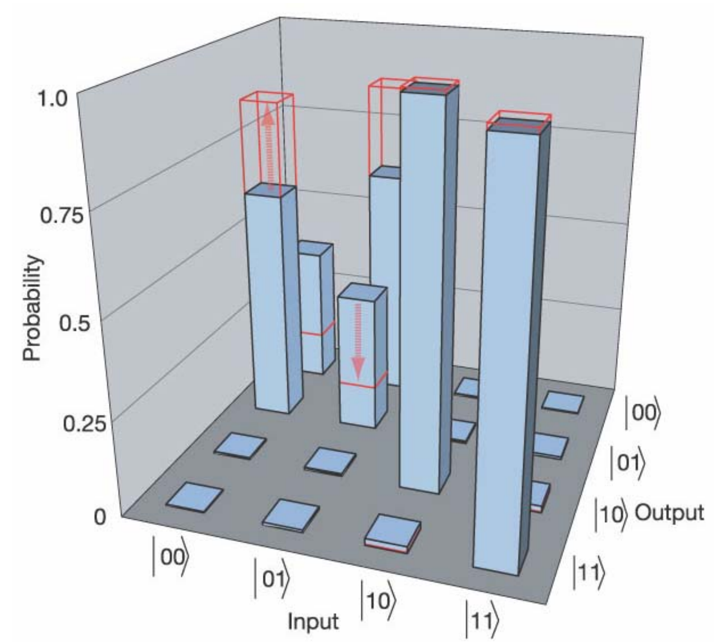

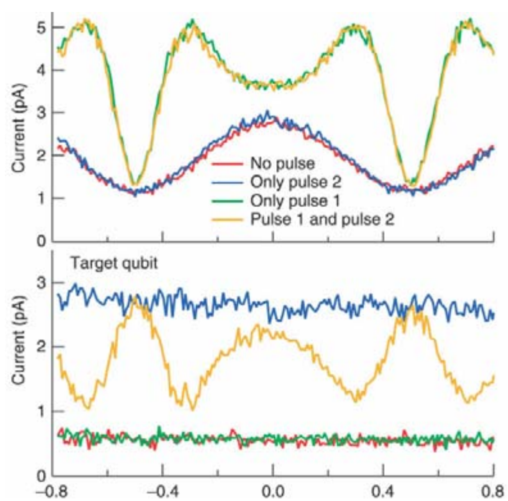

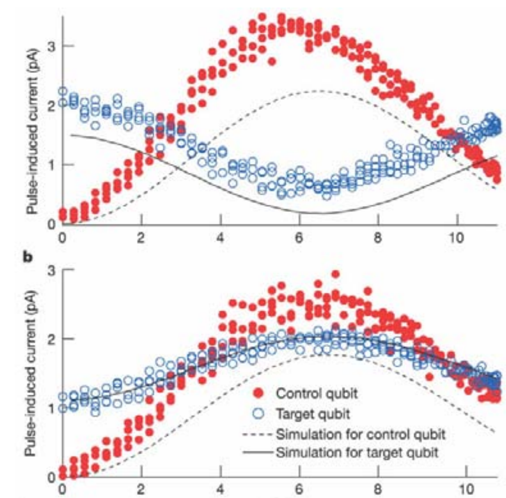

charge qubit with phase read-out

D. Vion, A. Aassime, A. Cottet, P. Joyez, H. Pothier, C. Urbina, D. Esteve, M.H. Devoret, Science 296, 886 (2002)

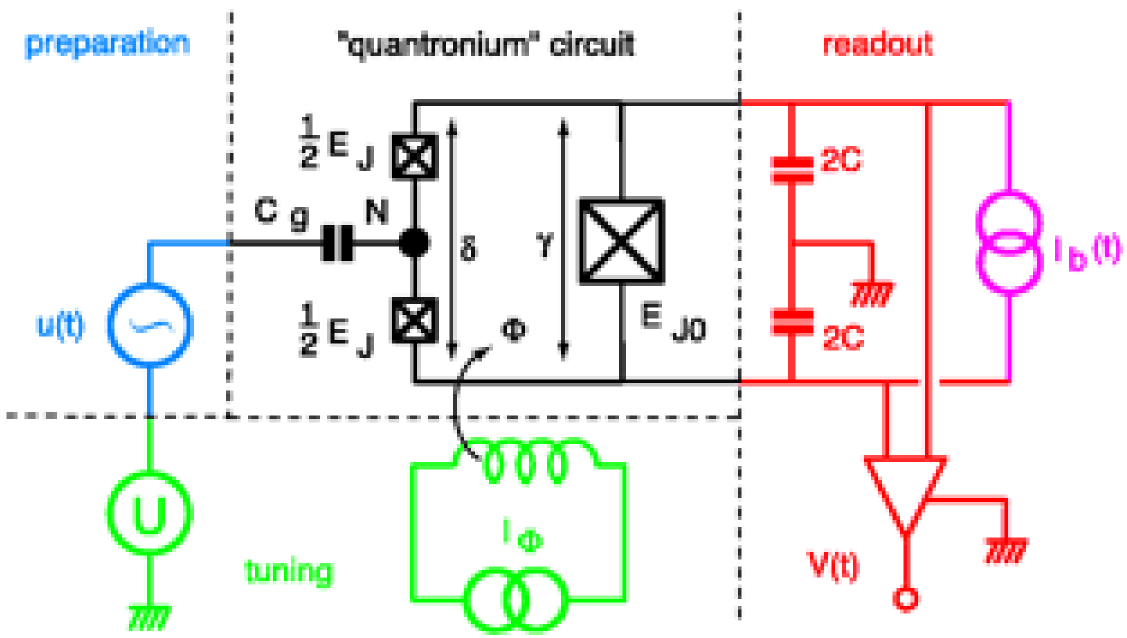

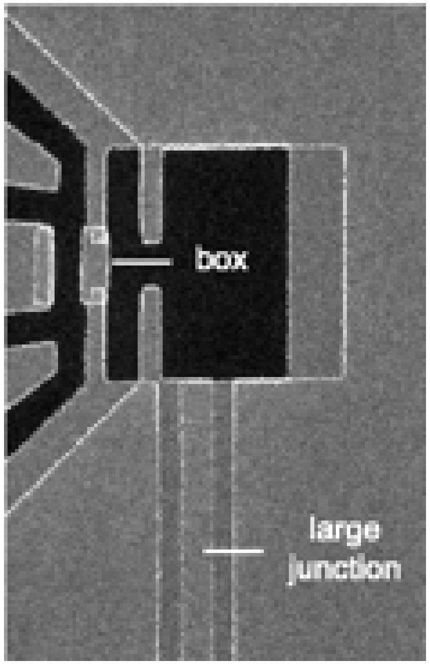

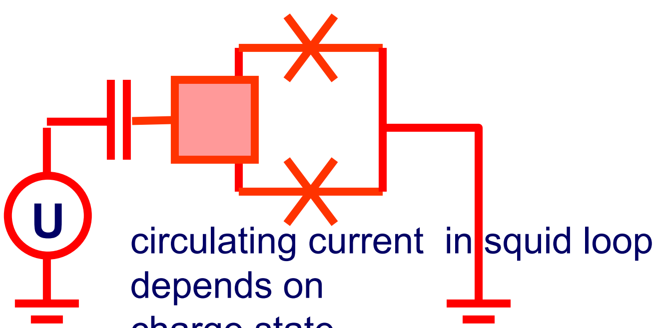

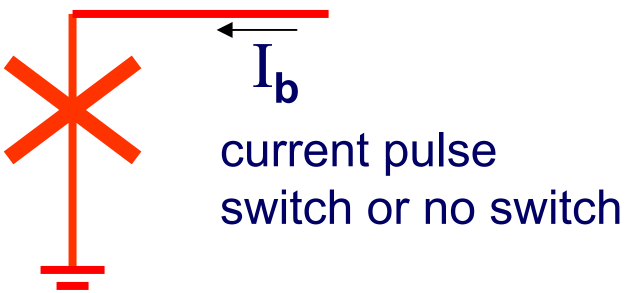

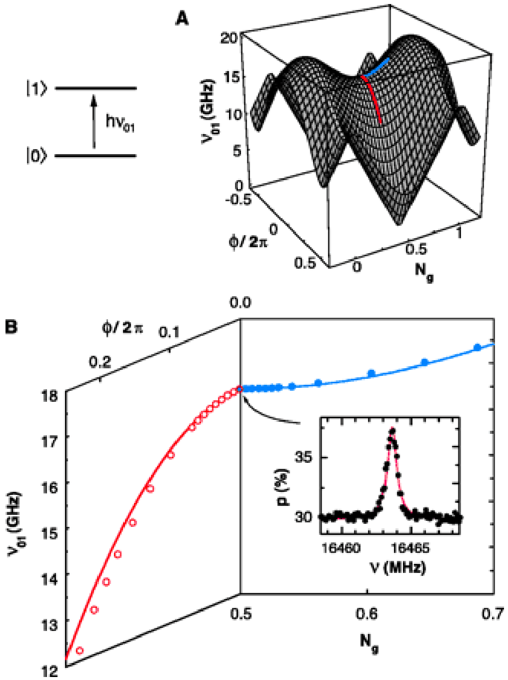
A
|1⟩
|0⟩
hν01
ν01 (GHz)
φ / 2π
Ng
B
φ / 2π
ν01 (GHz)
Ng
p (%)
ν (MHz)

'magic point'

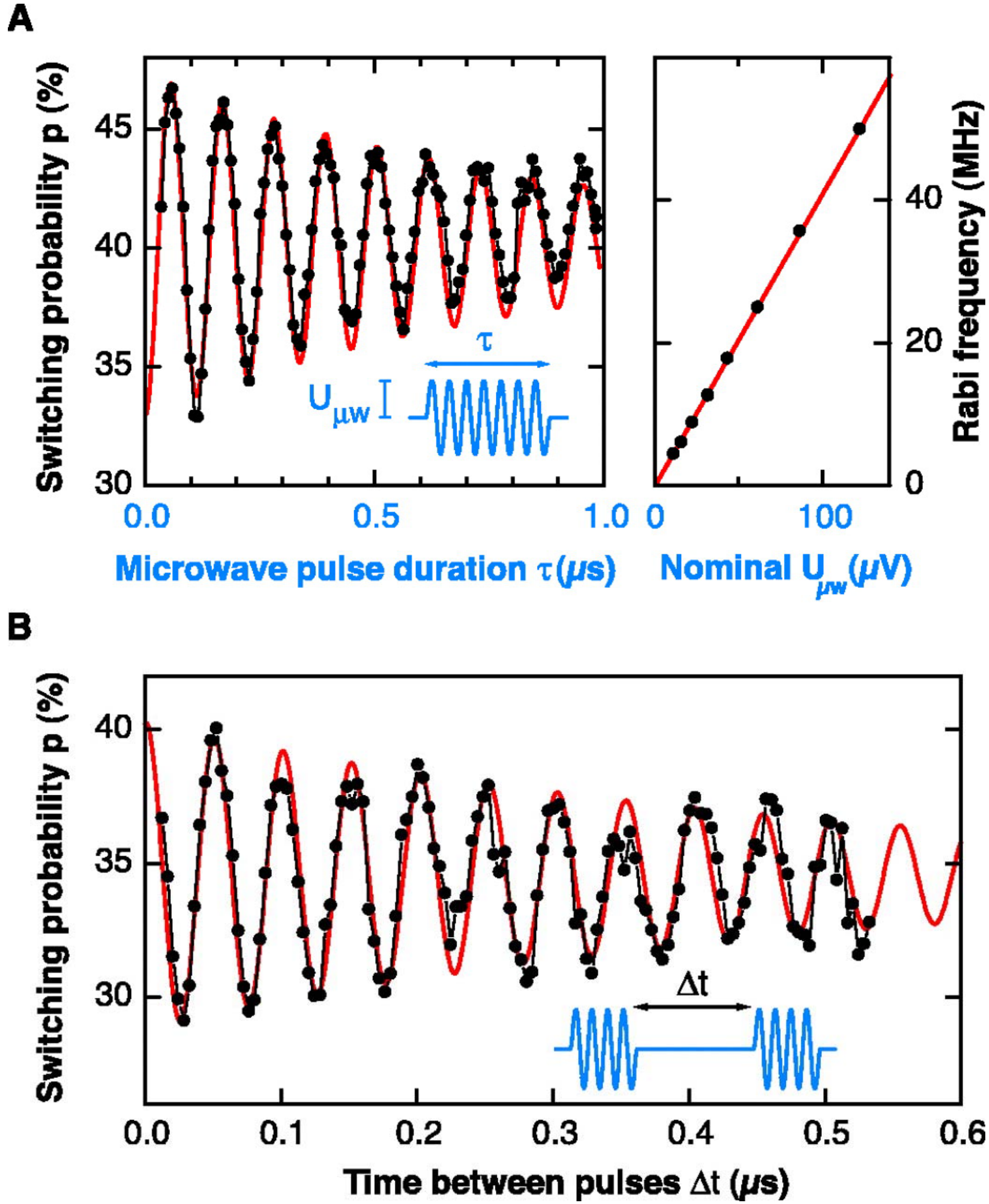
A
Switching probability p (%)
τ
Uμw
Microwave pulse duration τ (μs)
Nominal Uμw (μV)
Rabi frequency (MHz)
B
Switching probability p (%)
Δt
Time between pulses Δt (μs)

persistent-current quantum bit

flux qubit with three junctions, small geometric loop inductance

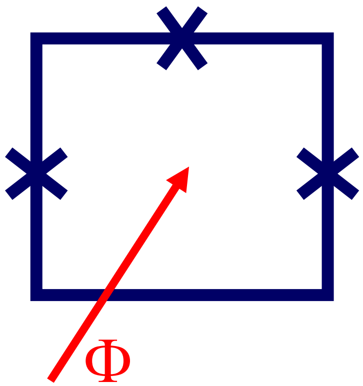

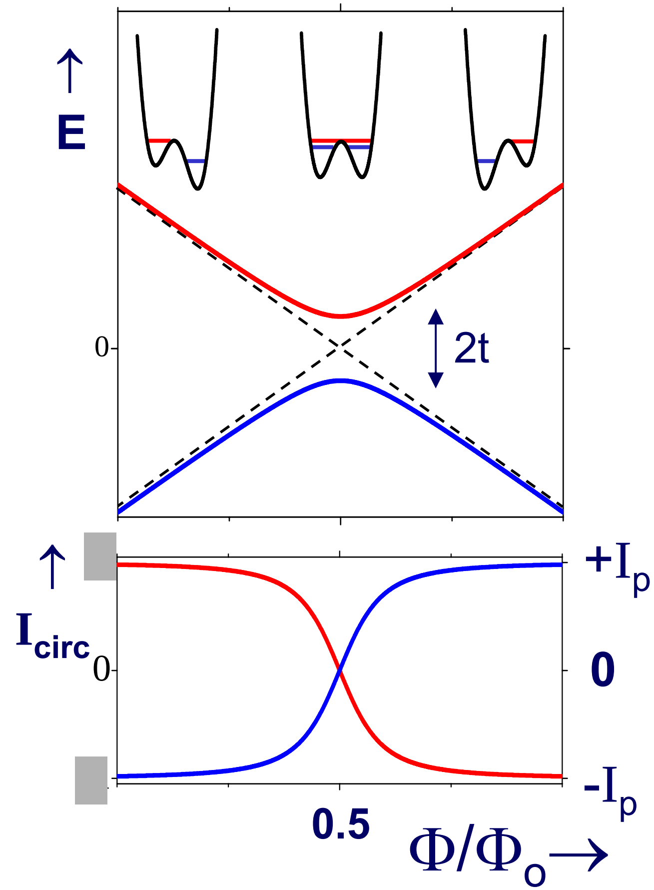

$H = h\sigma_z + t\sigma_x$

with $h=(\Phi/\Phi_o-0.5)\ \Phi_o I_p$

Science **285**, 1036 (1999)

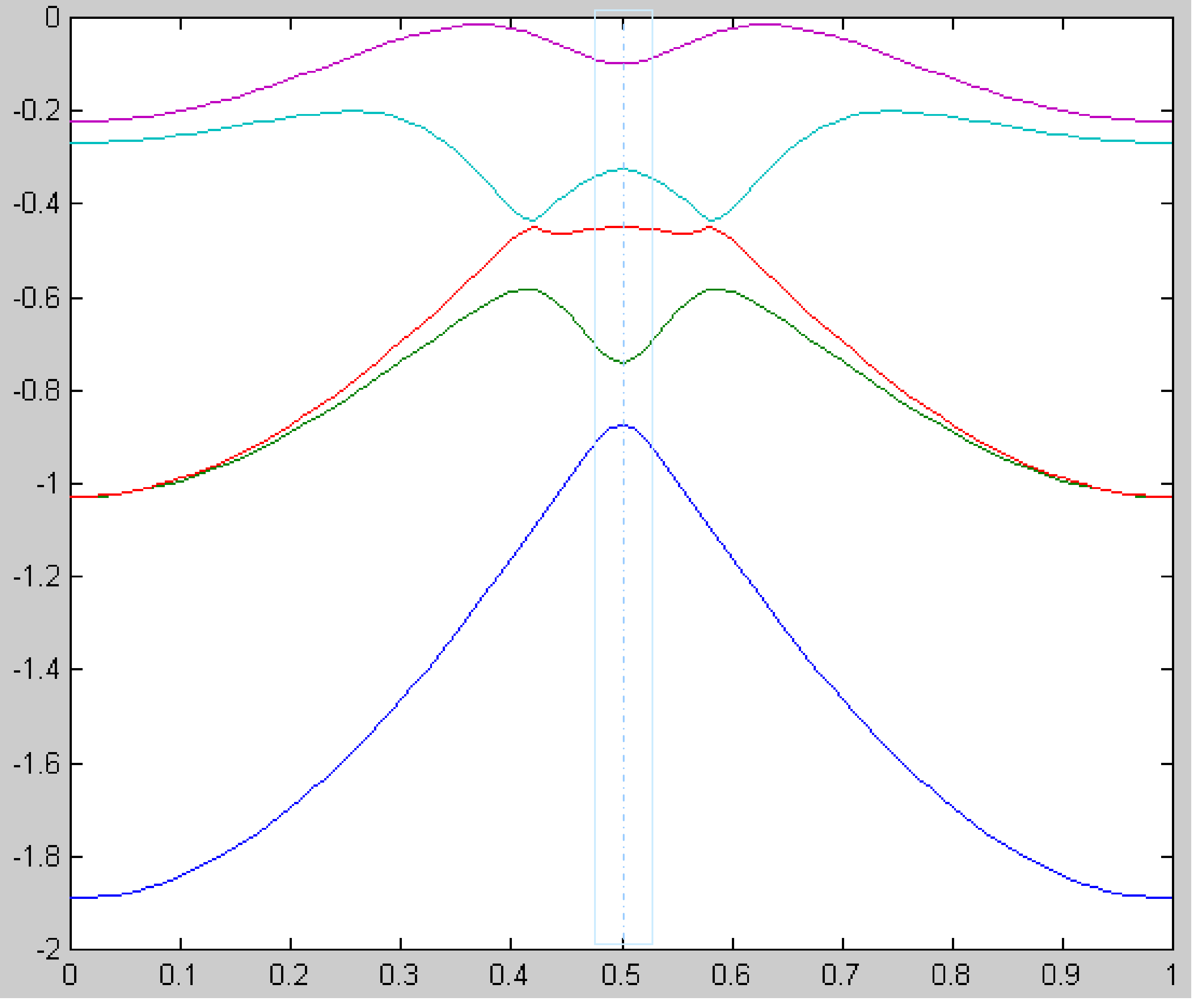

Φ/Φ_o

SQUID: $I_{s\ max}(\Phi)$

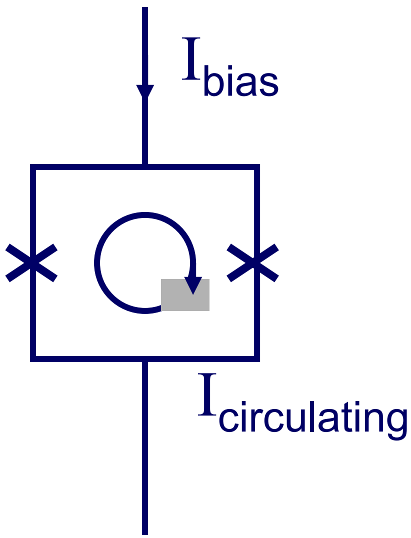

maximum supercurrent

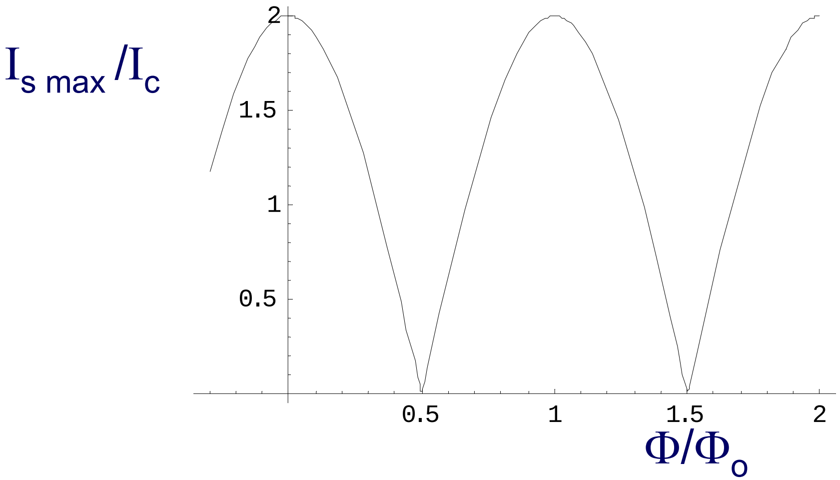

circulating current at f=0.5

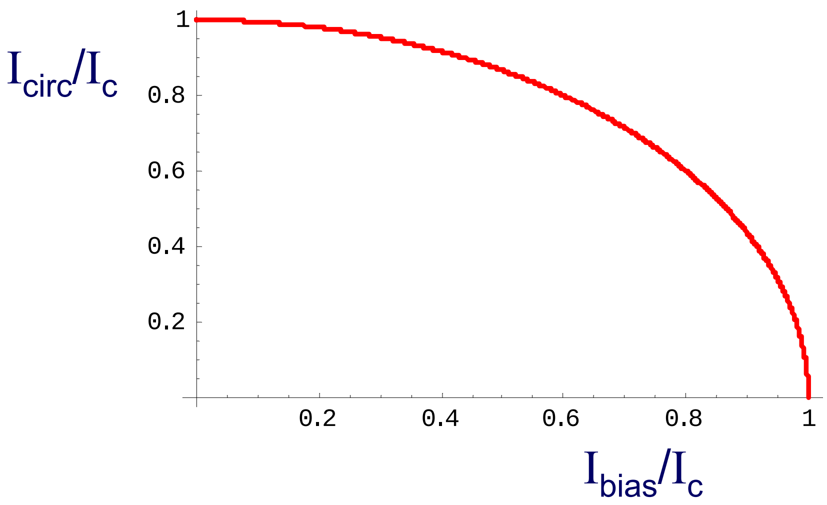

SQUID measurement

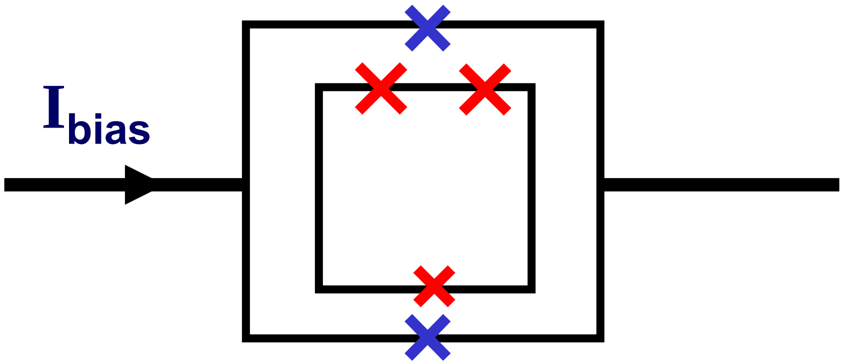

qubit generates flux $\pm LI_p \approx 10^{-3}\,\Phi_o$
measured with
hysteretic (unshunted) SQUID
maximum supercurrent depends on
flux in the SQUID loop

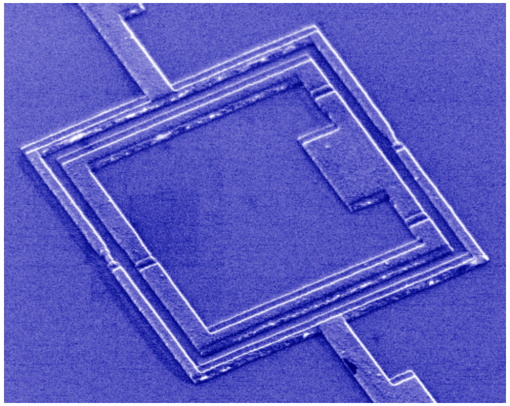

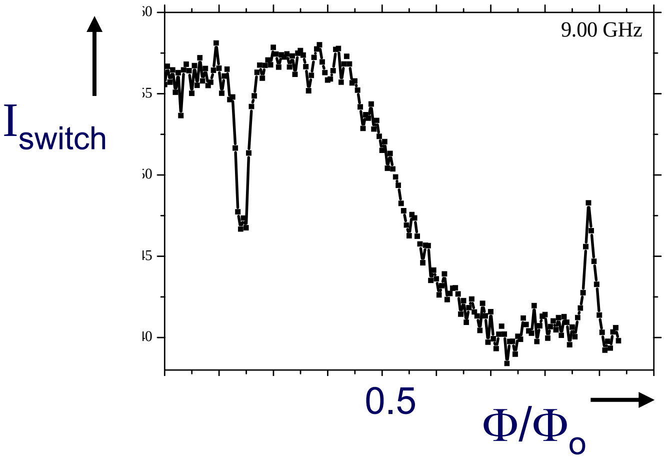

measurement switching current:
(RF 9 GHz applied)
5000-10000 ramps

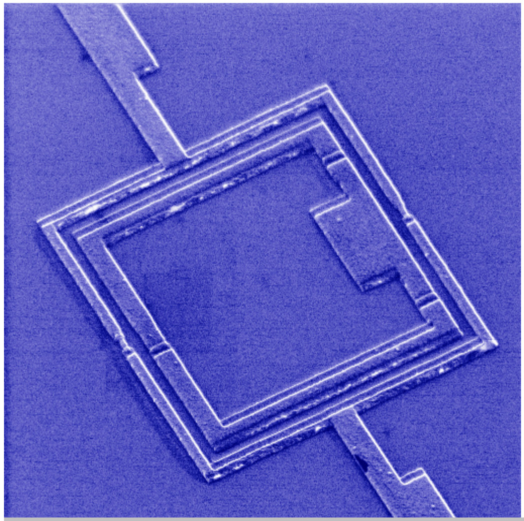

SQUID I_c 200 nA

underdamped, no ohmic shunt

measurement of I_{switch}

by repeated ramping

histogram of 5,000-10,000 points

average value recorded

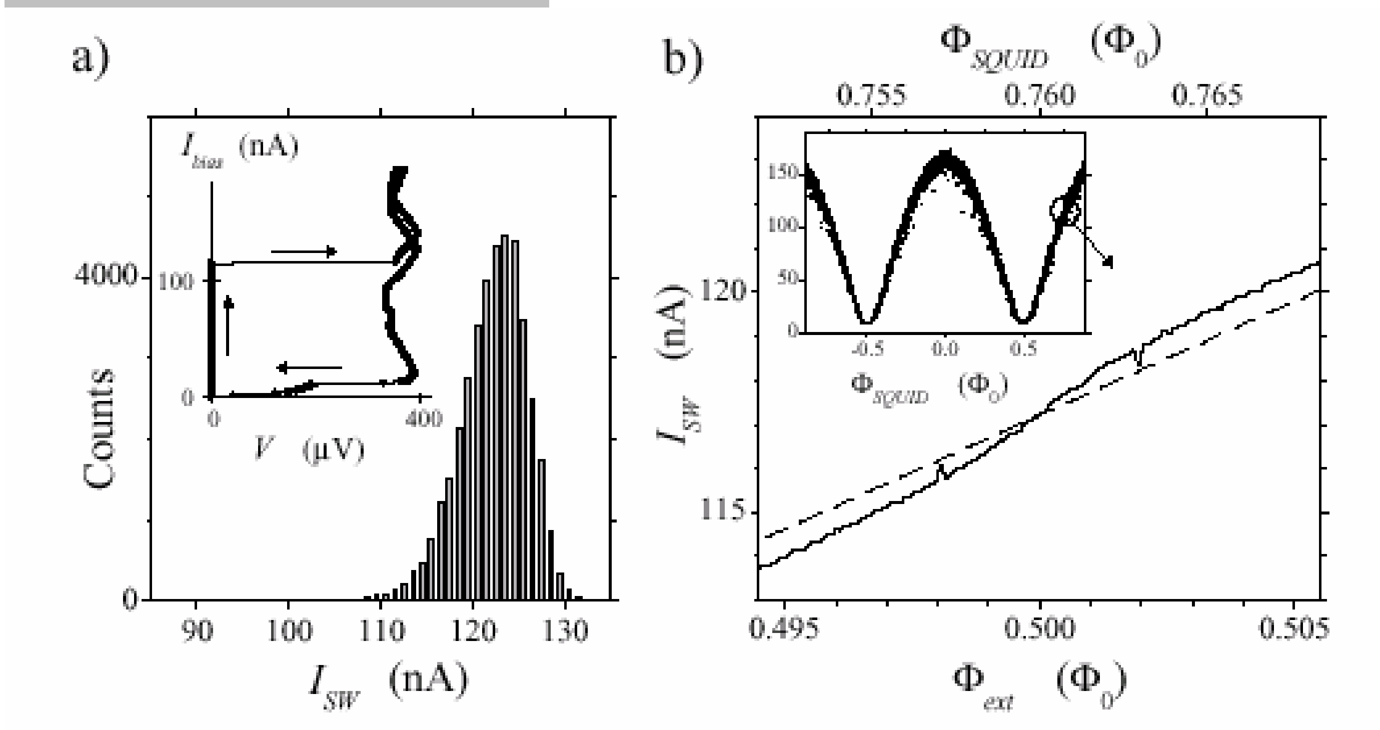

superposition of states with clockwise and anti-clockwise-current

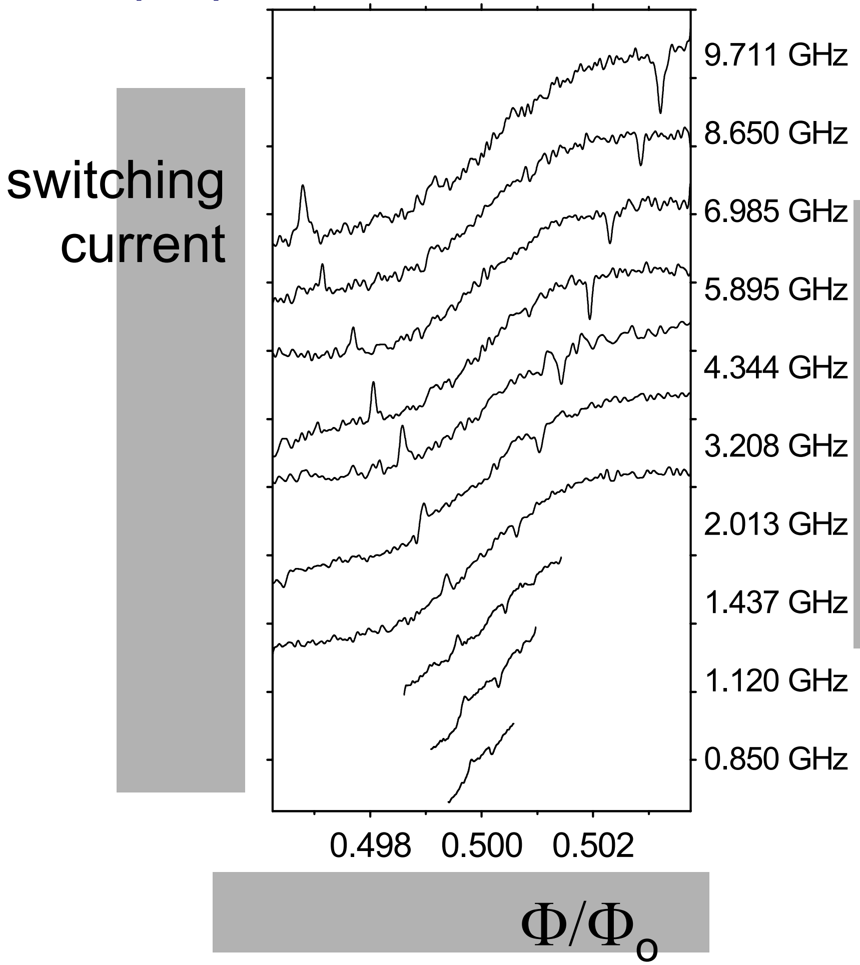

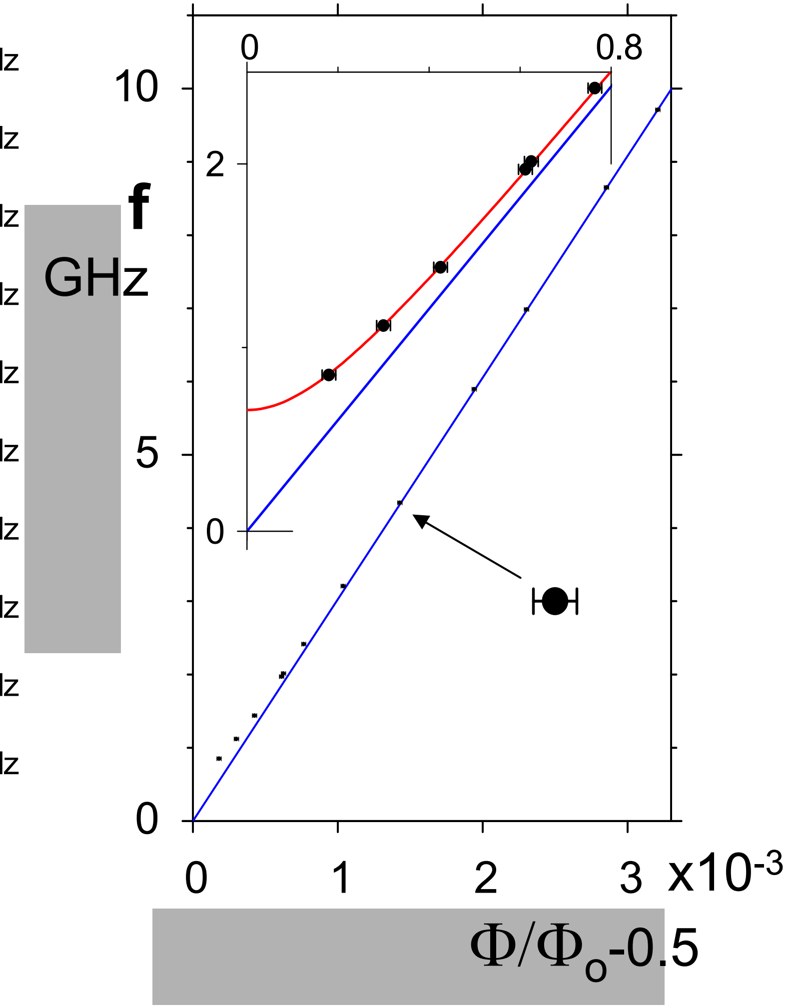

Van der Wal et al., Science 290, 773 (2000)

also SUNY (Friedman, Lukens et al.)

Friedman, Patel, Chen, Tolpygo, Lukens: Nature **406**, 43 (2000)

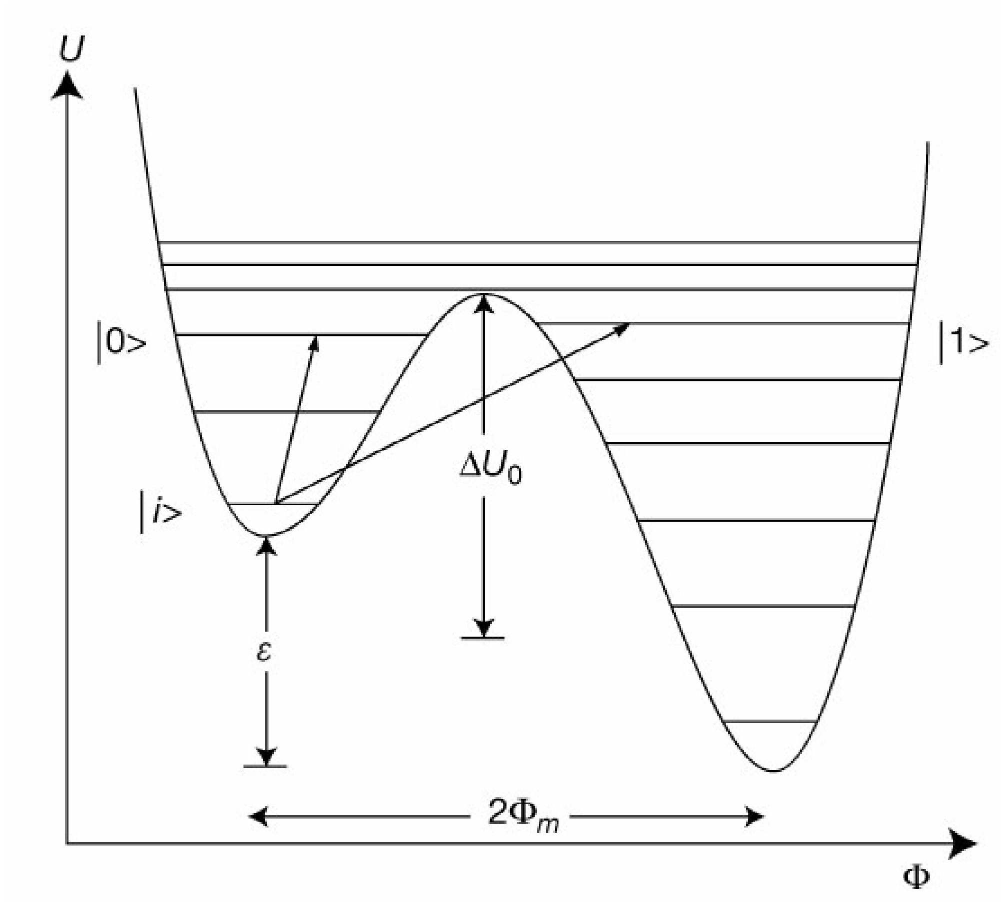

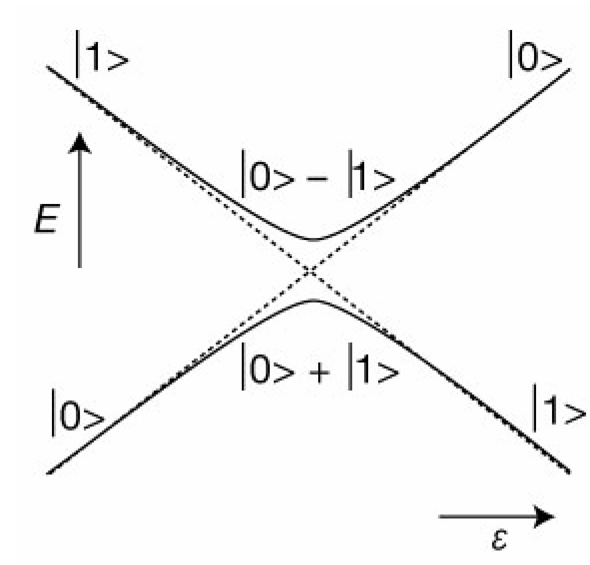

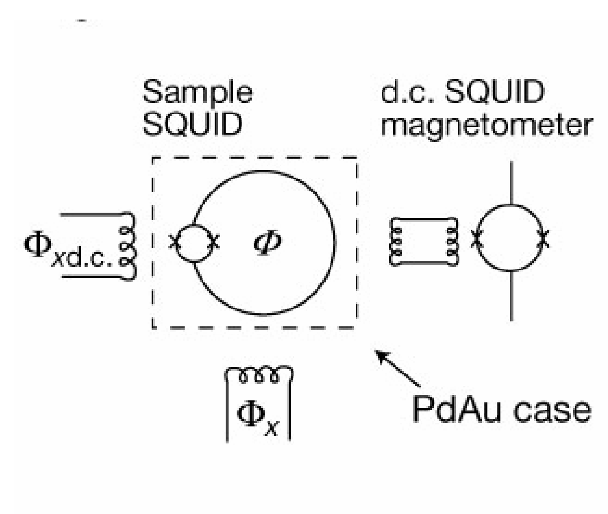

ΔE and E_B manipulated with flux

E_J=76 K ($\cos\Phi_{xdc}/\Phi_o$), E_C= 9 mK

ΔU_o= 9 K

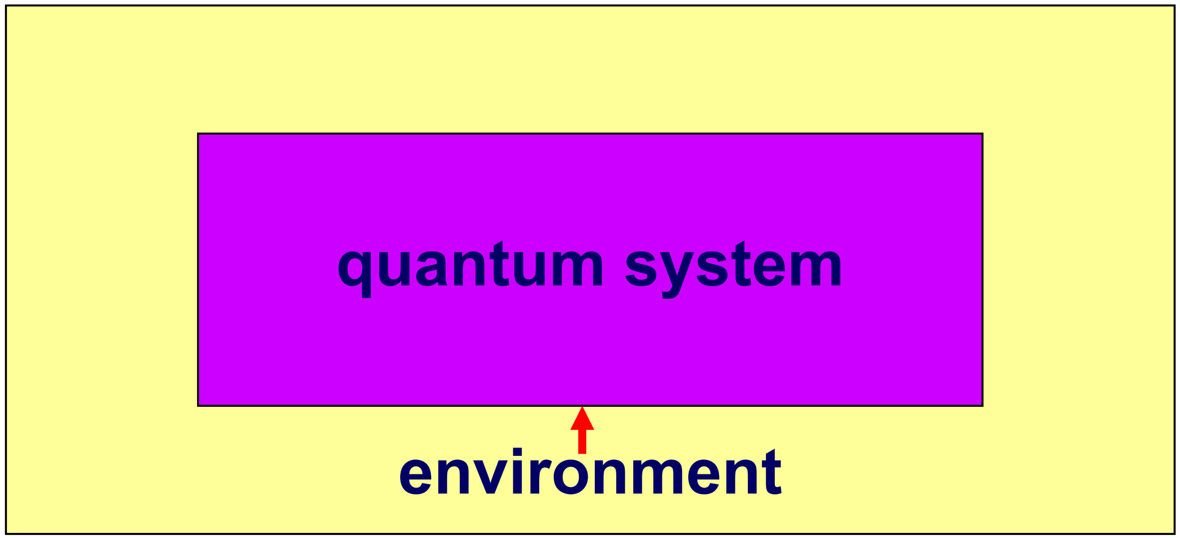
quantum system
environment

Decoherence

relaxation T_1 τ_{relax} dephasing T_2 τ_ϕ

- pseudospin - boson bath (harmonic oscillators)

Milena Grifoni, Frank Wilhelm, Gerd Schon et al

τ_{relax} determined by spectral density at ΔE

τ_ϕ determined by spectral density at low ω

measurement circuit designed to optimize

- pseudospin - spin bath ? $\rightarrow$ Phil Stamp

- 1/f type noise: flux, charge, critical current

1/f noise

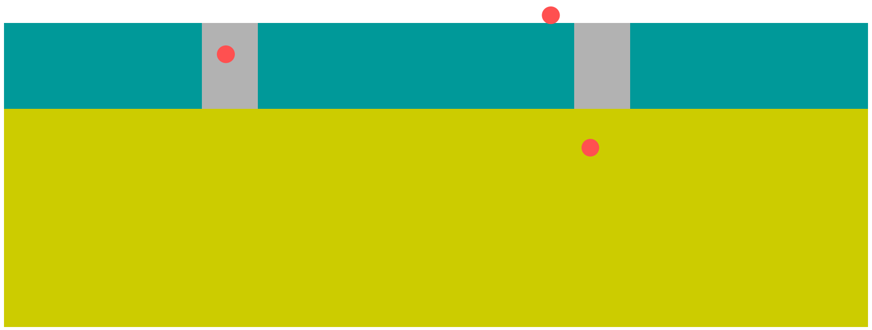

- charge noise: charged defects in barrier, substrate or surface lead to non-integer induced charge. Static offset, 1/f noise.

- critical current noise: neutral defects in barrier.

- flux noise: trapped vortices, magnetic domains, magnetic impurities, nuclear spins

Delft flux qubits

Kees Harmans
Alexander ter Haar
Irinel Chiorescu
Adrian Lupascu
Floor Pauw
Patrice Bertet
Jelle Plantenga
Jonathan Eroms
Yasunobu Nakamura (NEC)
Kouichi Semba (NTT)

funding: FOM, EU
ARO, Kavli

h set by external flux

t set by fabrication

excitation, measurement σ_z

$$H = h\sigma_z + t\sigma_x$$

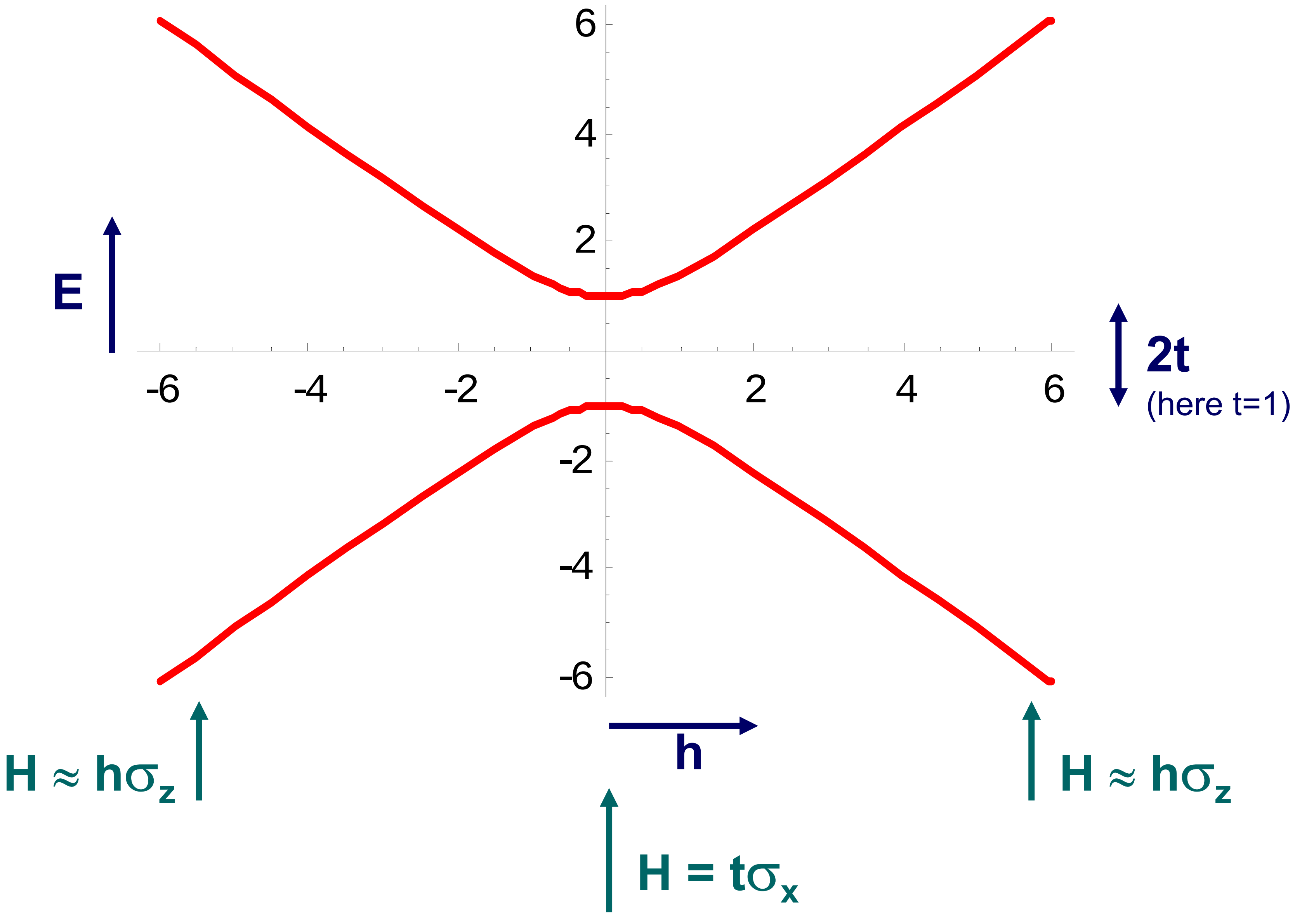

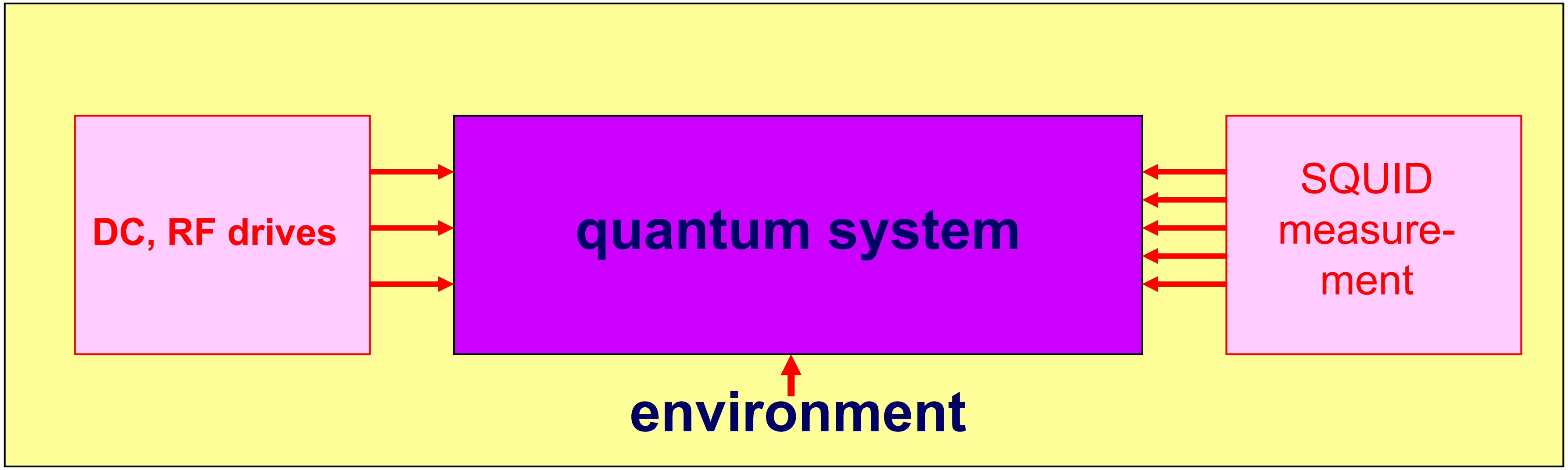
DC, RF drives
quantum system
SQUID
measure-
ment
environment

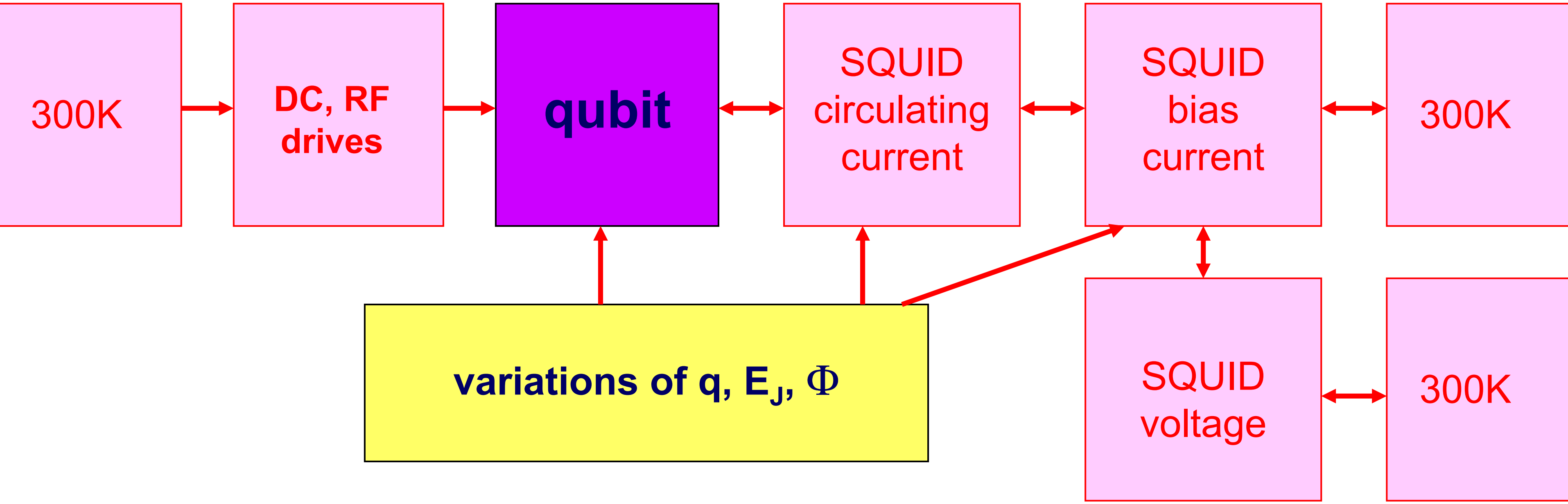

300K
DC, RF drives
qubit
SQUID circulating current
SQUID bias current
300K
variations of q, E_J, Φ
SQUID voltage
300K

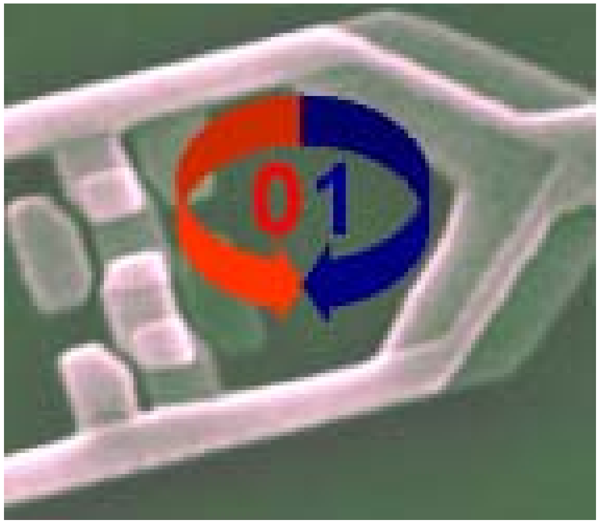

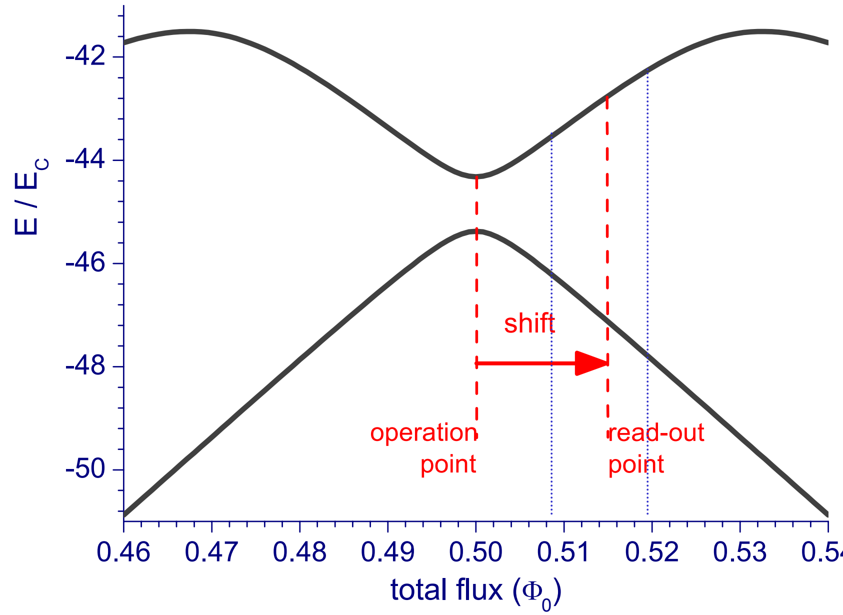

intended principle:
- quantum operations at symmetry point where $dE/d\Phi=0$ (but also qubit circulating currents are zero)
- use changing SQUID circulating current for automatic shift to a read-out bias where there is qubit current to measure

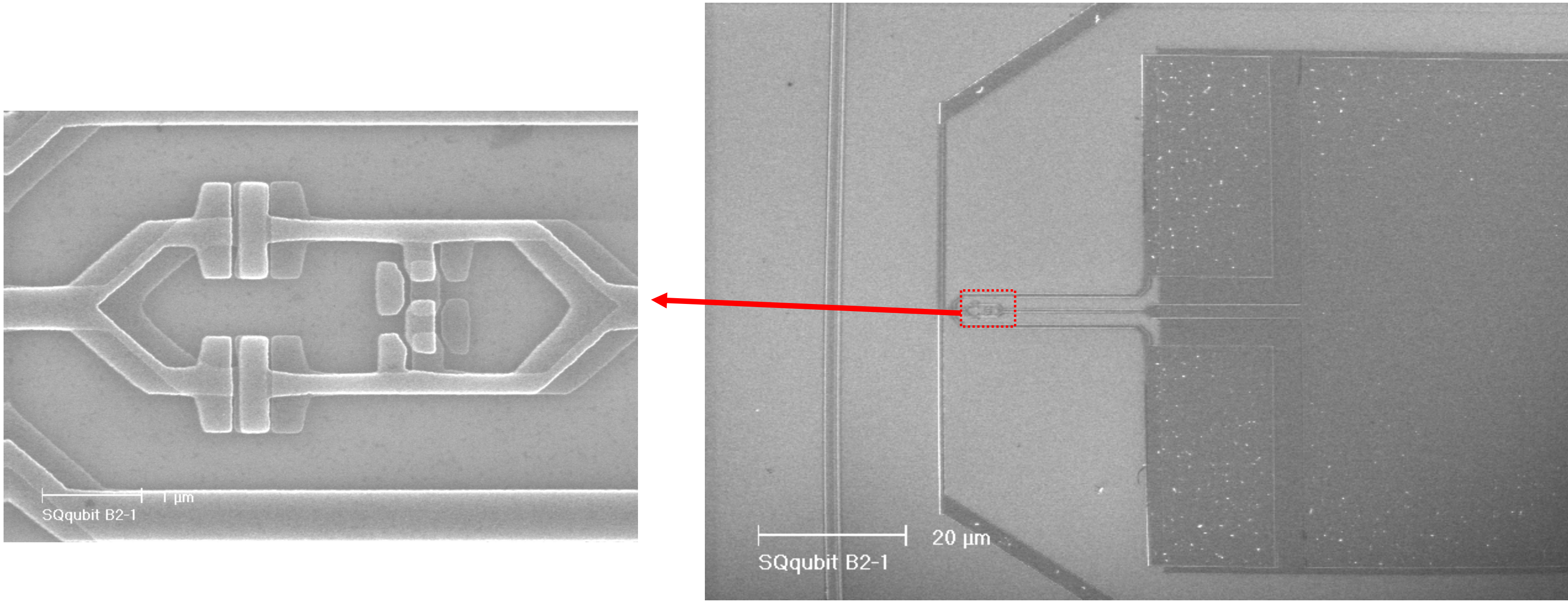

well-designed electromagnetic environment

calculated $T_1 = 100\ \mu s$

$T_2 = 20\ \mu s$

operation time 1 ns

SQUID shunted by large capacitance on chip

SQUID readout:

only two possible outputs:

SQUID switched to gap voltage

SQUID still at V=0

pulse height adjusted to give ~50% switching

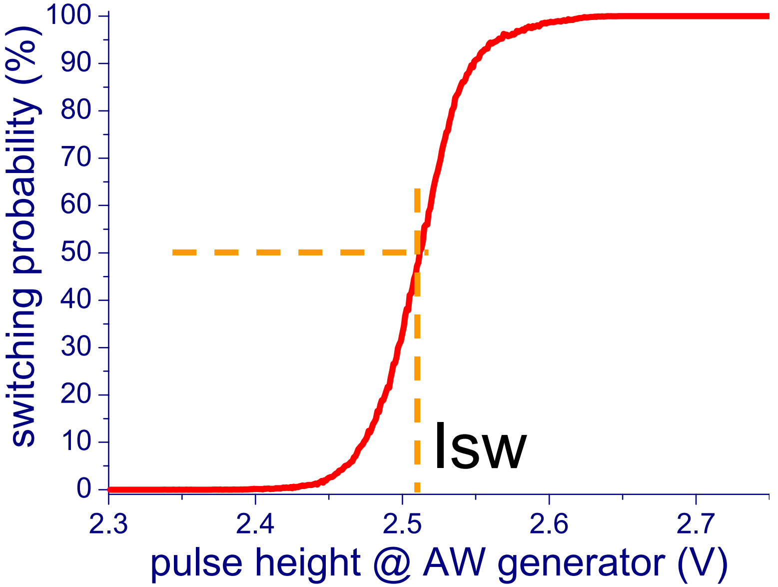

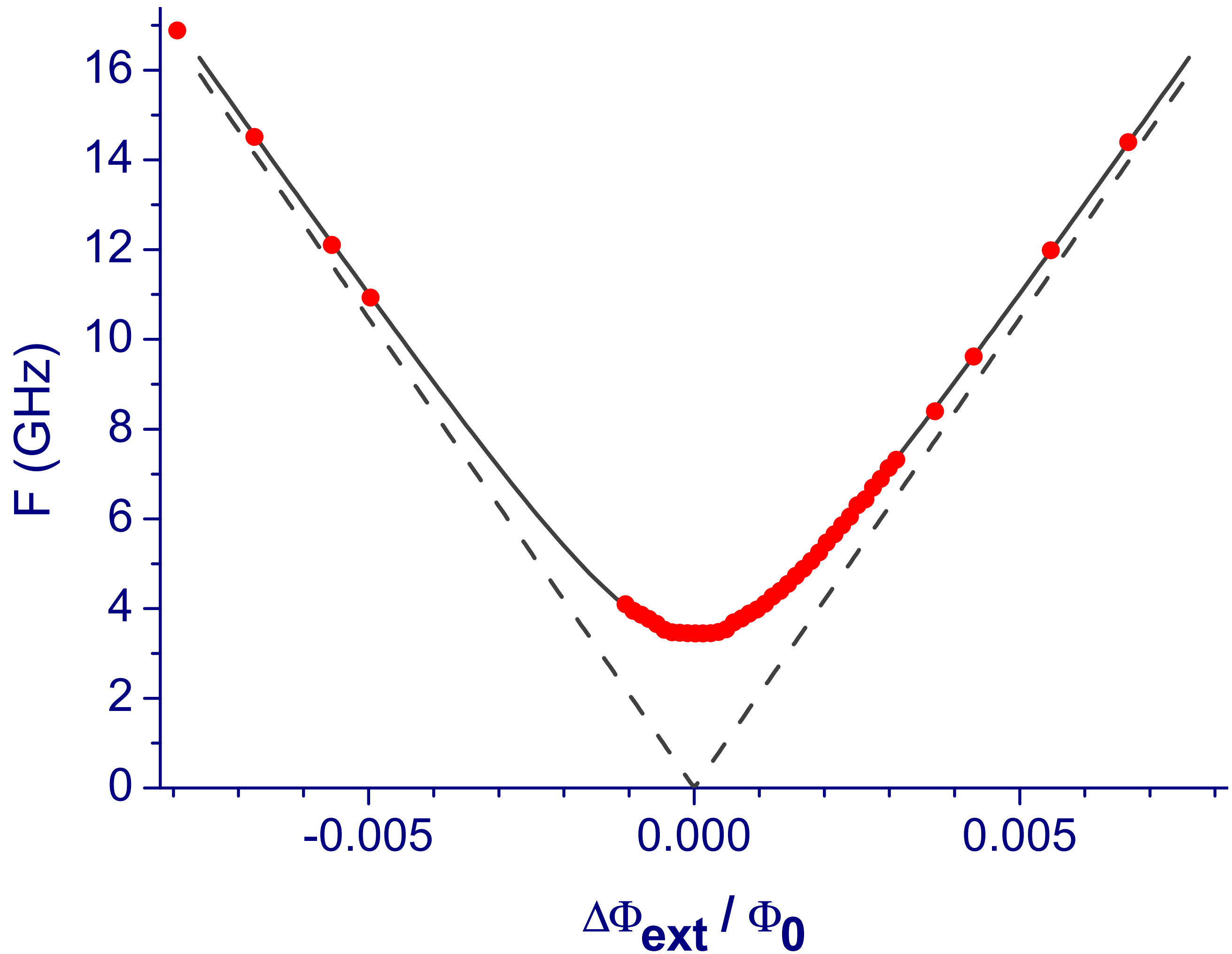

16
14
12
10
8
6
4
2
0
F (GHz)
-0.005
0.000
0.005
ΔΦext / Φ0

Rabi: microwave pulse with varying length

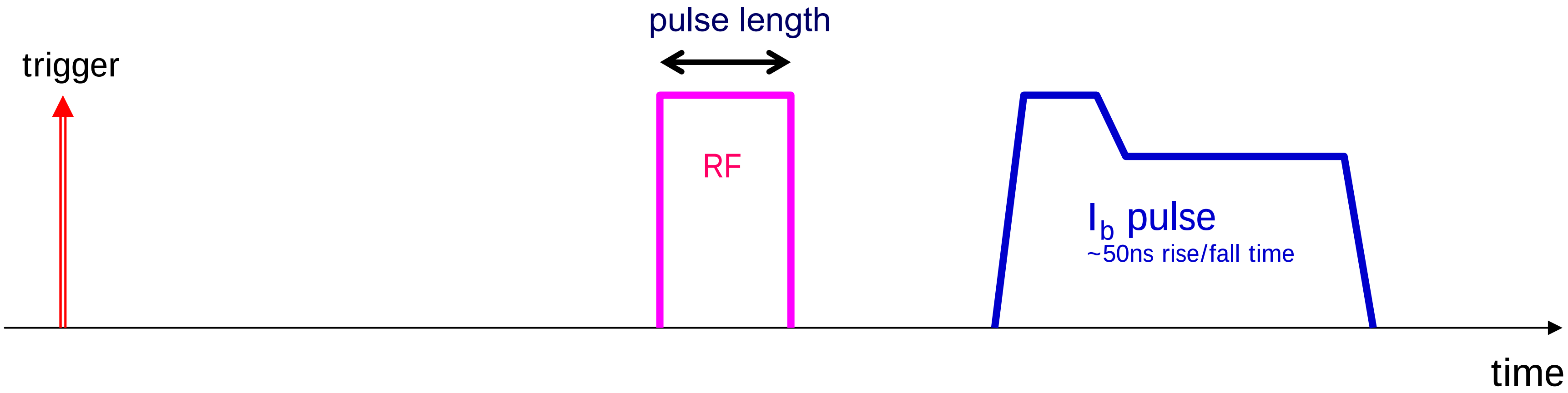

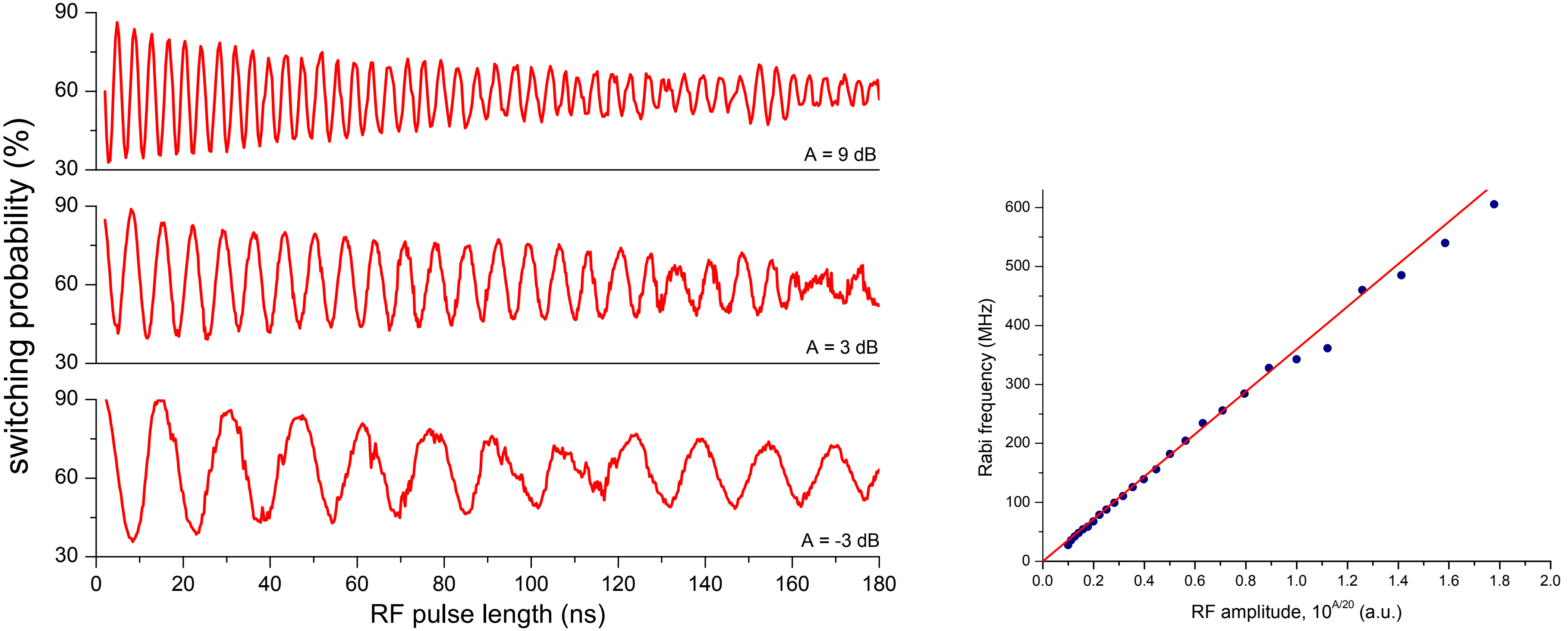

switching probability (%)
90
60
30
A = 9 dB
A = 3 dB
A = -3 dB
0
20
40
60
80
100
120
140
160
180
RF pulse length (ns)
Rabi frequency (MHz)
0
100
200
300
400
500
600
0.0
0.2
0.4
0.6
0.8
1.0
1.2
1.4
1.6
1.8
2.0
RF amplitude, 10^A/20 (a.u.)

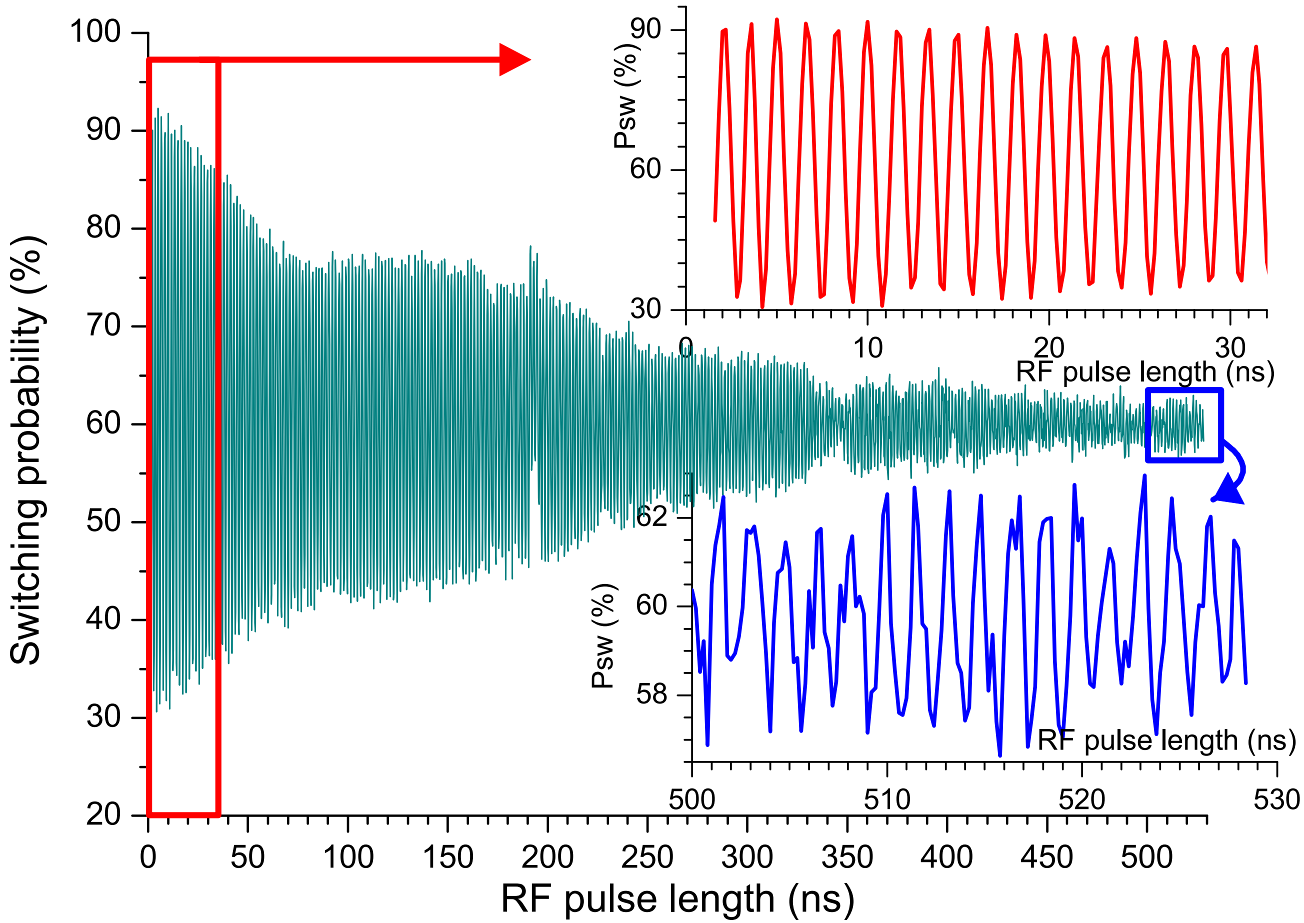

Switching probability (%)
RF pulse length (ns)
100
90
80
70
60
50
40
30
20
0
50
100
150
200
250
300
350
400
450
500
Psw (%)
90
60
30
0
10
20
30
RF pulse length (ns)
Psw (%)
62
60
58
500
510
520
530
RF pulse length (ns)

measurement of relaxation time
observed values: 40 ns to 300 μs

one π pulse and read-out pulse delayed

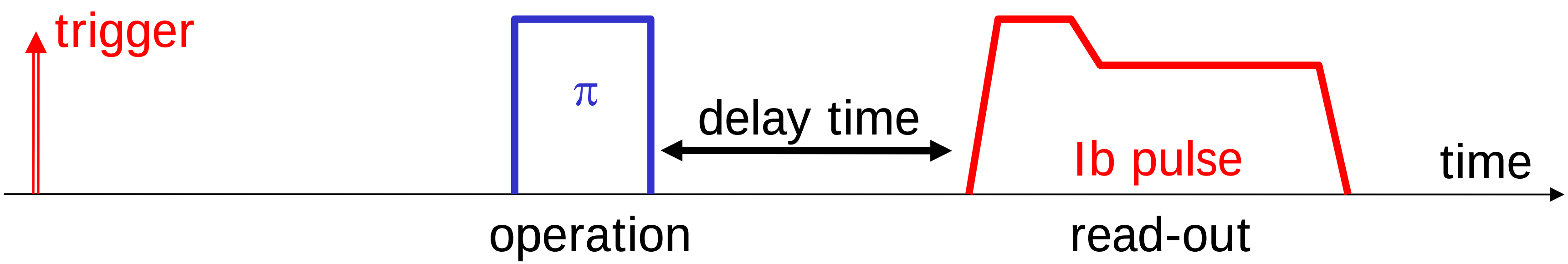

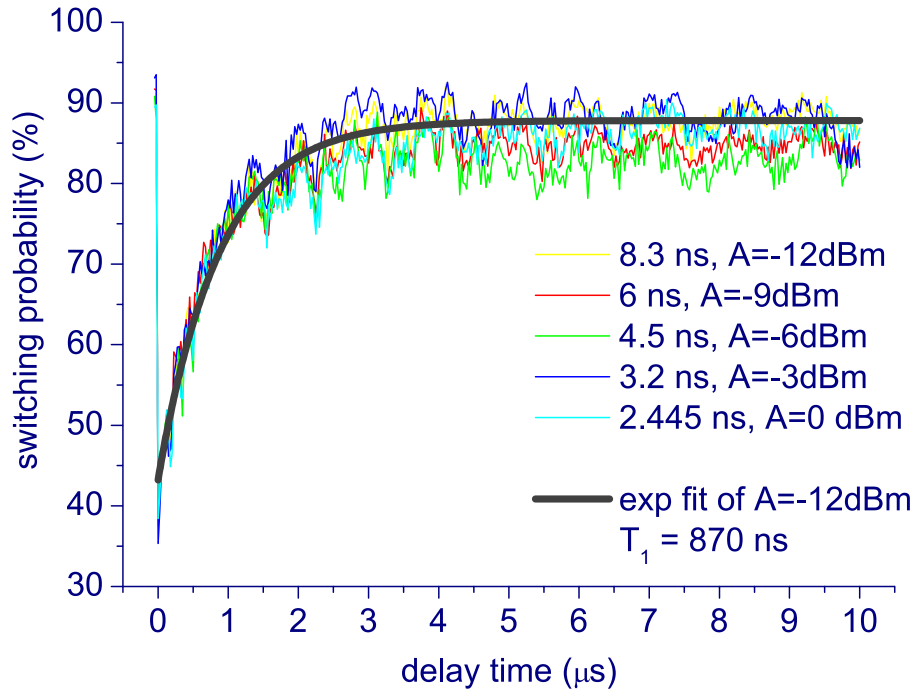

measurement T_2 time
Ramsey

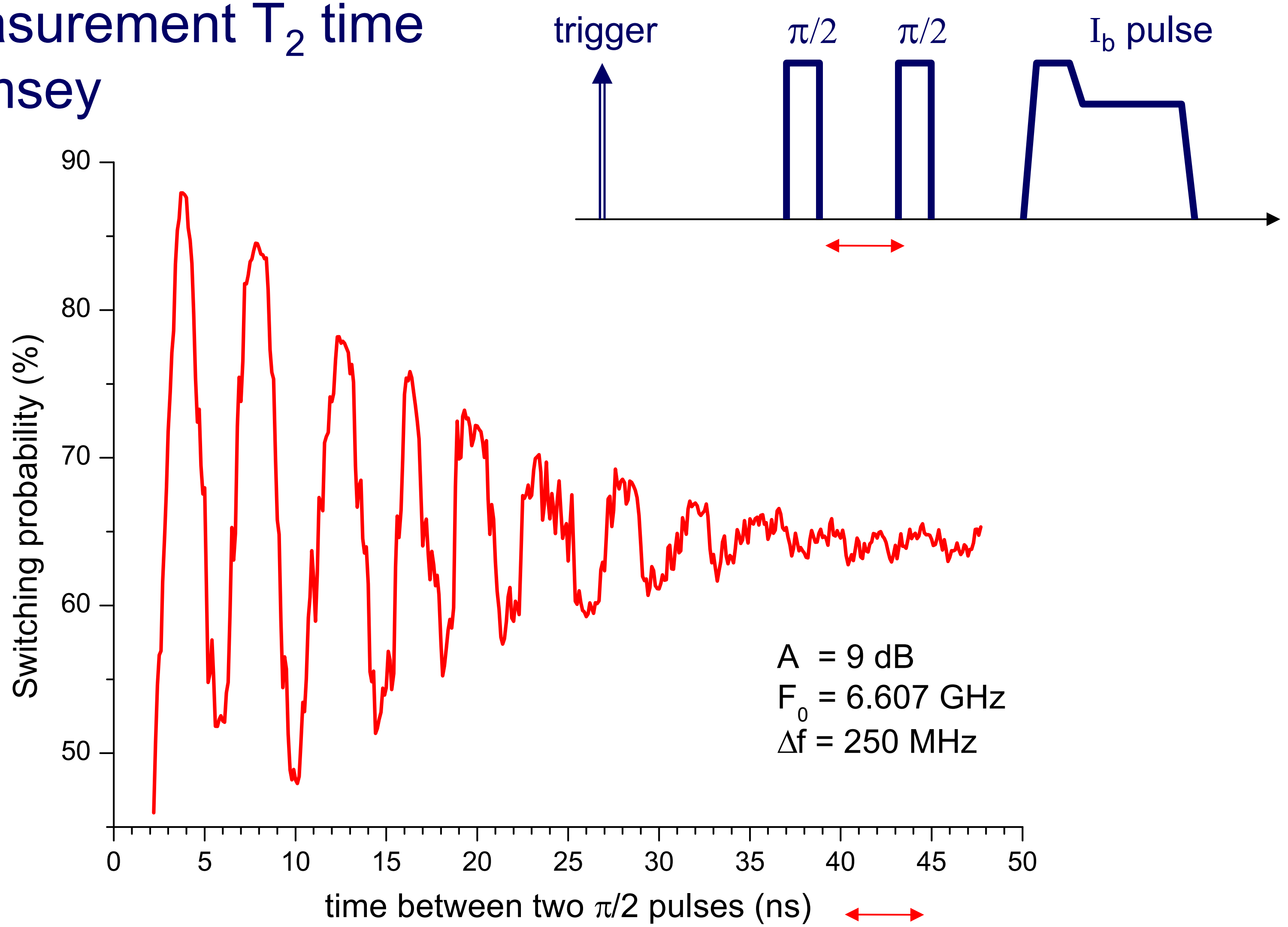

spin echo

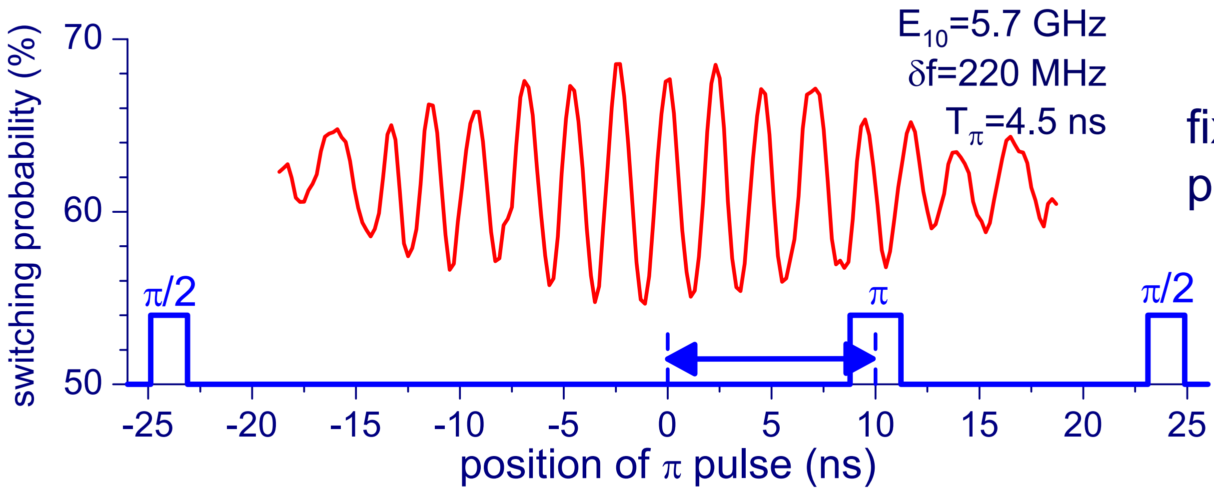

fixed time between $\pi/2$ pulses, π pulse shifting

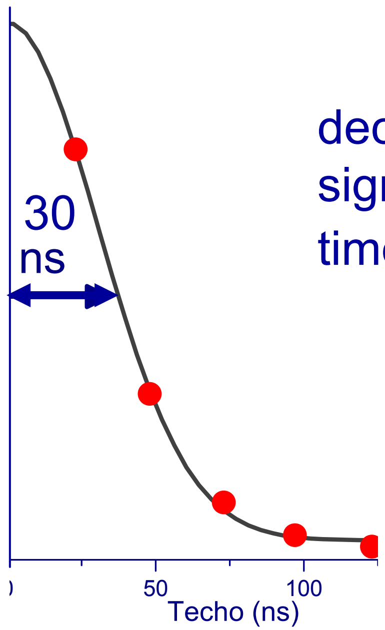

decay of maximum spin echo signal versus
time between $\pi/2$ pulses

T_2 (higher frequencies)
30 ns

Rabi with low number of measurements, single shot contains some information

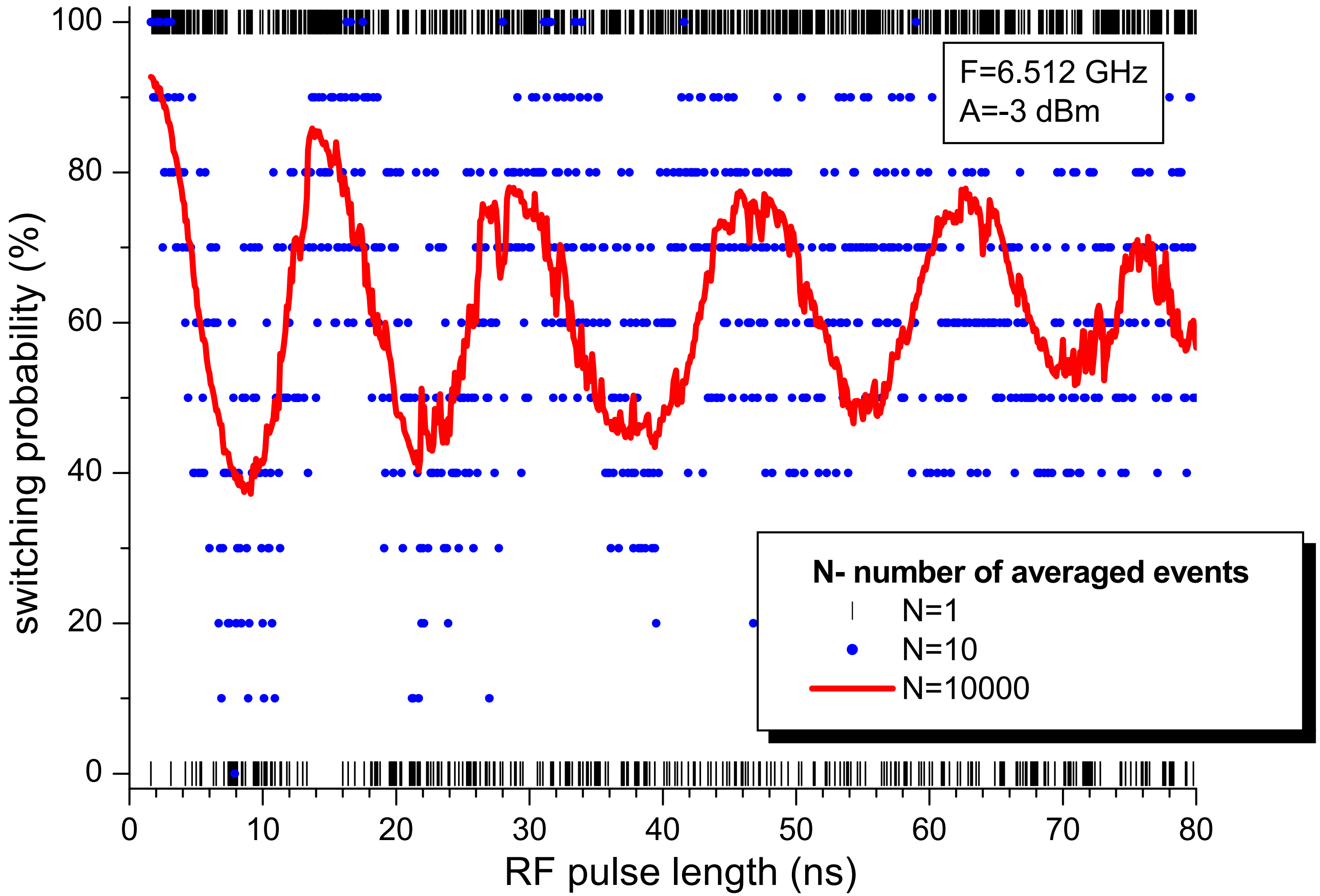

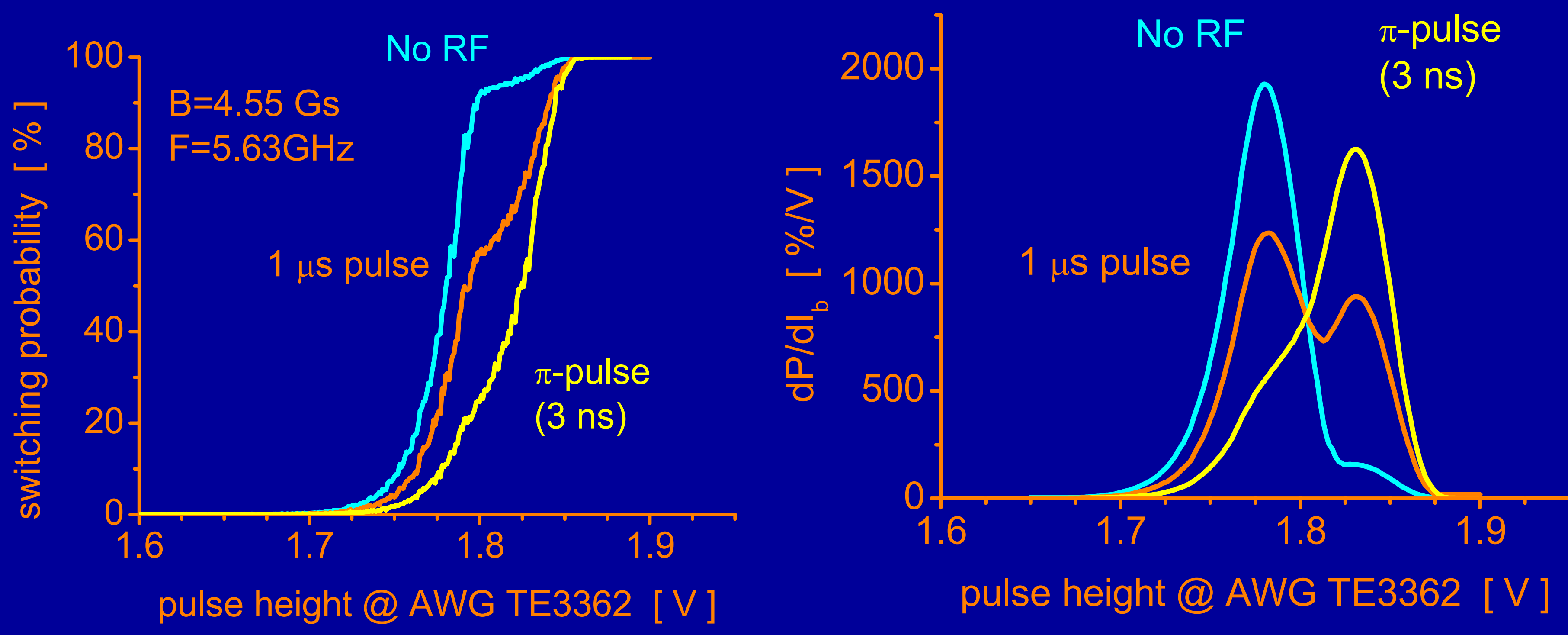

Kouichi Semba, NTT, Delft

TE3362 AWG

inductive readout, circuit

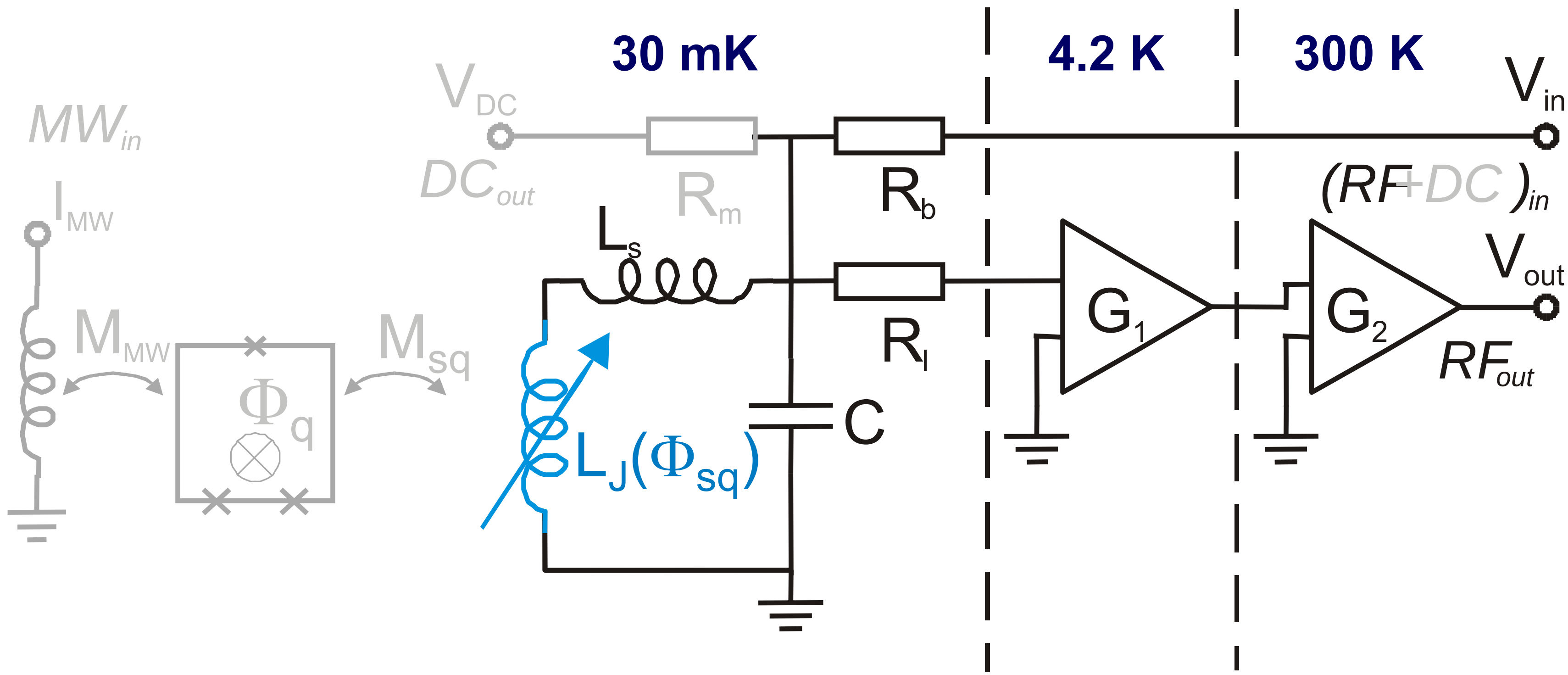

circuit parameters

C = 12 pF
L_s ~ 2.5 nH
R_L = 820 W
R_b = 5.6 kW
R_m = 11 kW
Q~40

Adrian Lupascu, Kees Harmans, Raymond Schouten

resonance curve

at B=0: F_{res}= 762.2 MHz, Q = 33

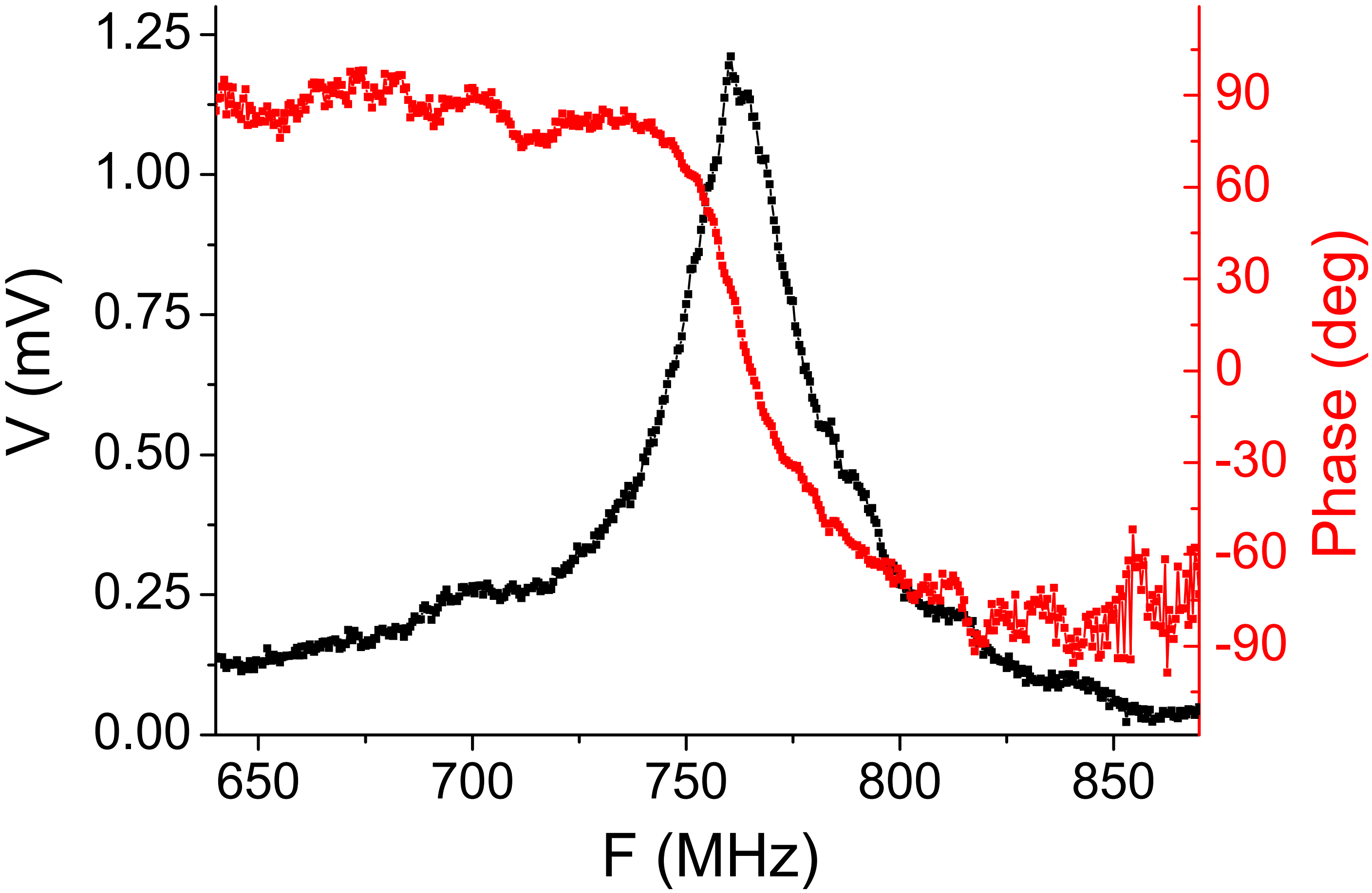

Typical spectroscopy curve

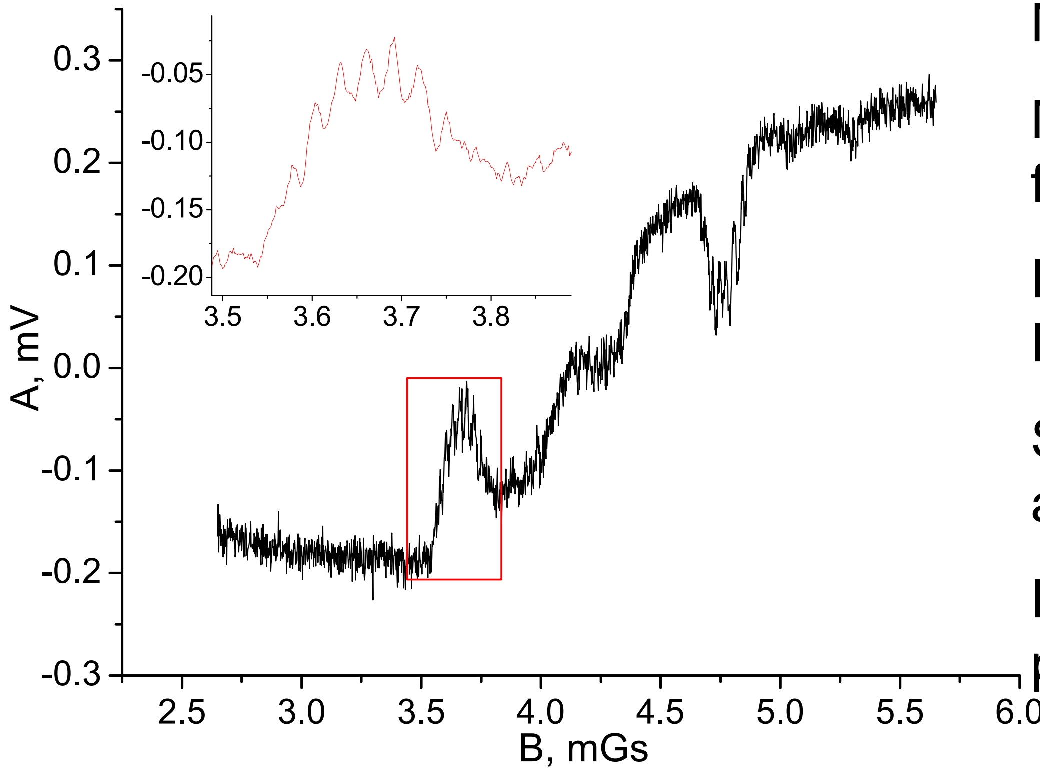

Measurements at step s1

Measurement scheme: 1μs MW followed by 2 μs readout pulse

F_{MW}=17 GHz, F_{IM}=855 MHz, F_{res}=838 MHz

SQUID excitation: current amplitude less that $1/2I_c$

Estimated sub-peaks period:750 MHz

relaxation

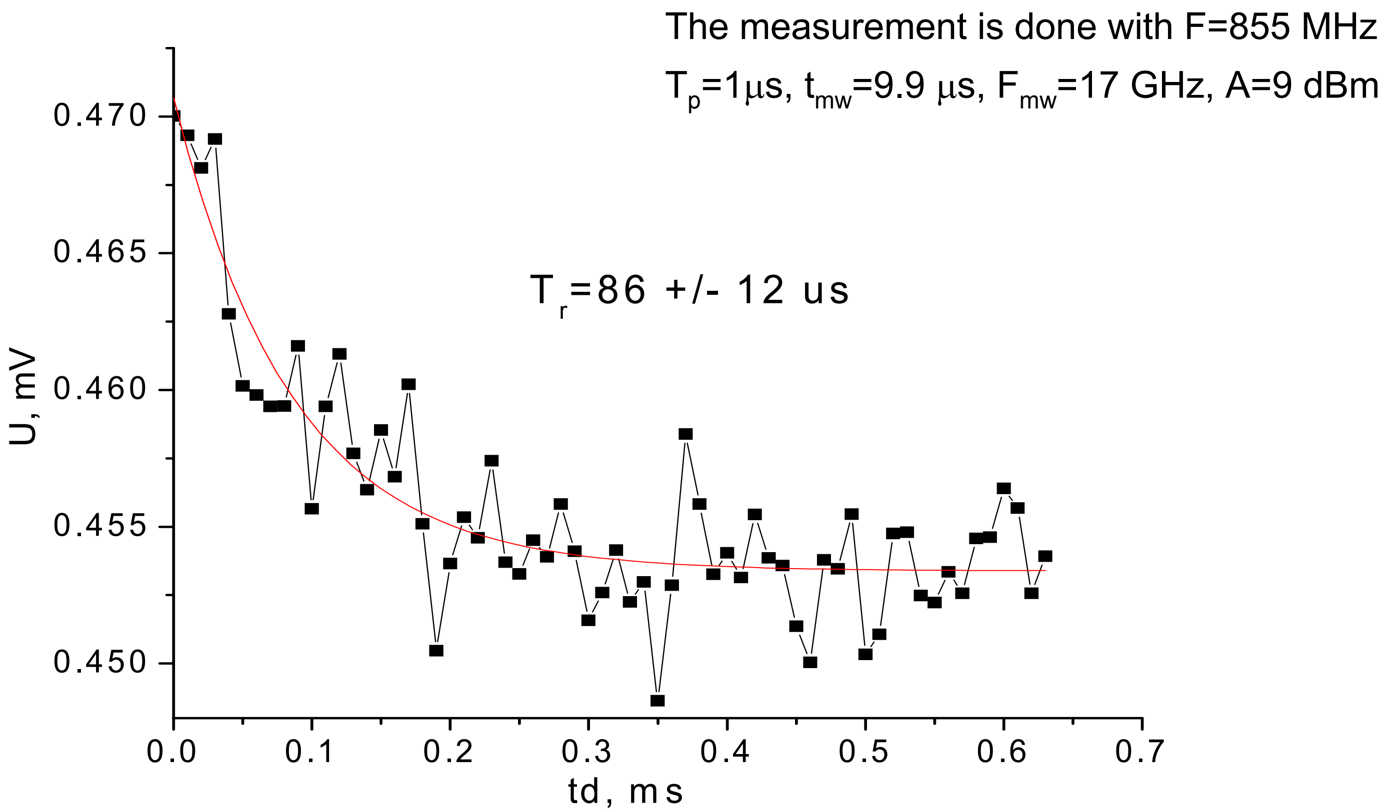

(preliminary) conclusion: relaxation time about 60 μs

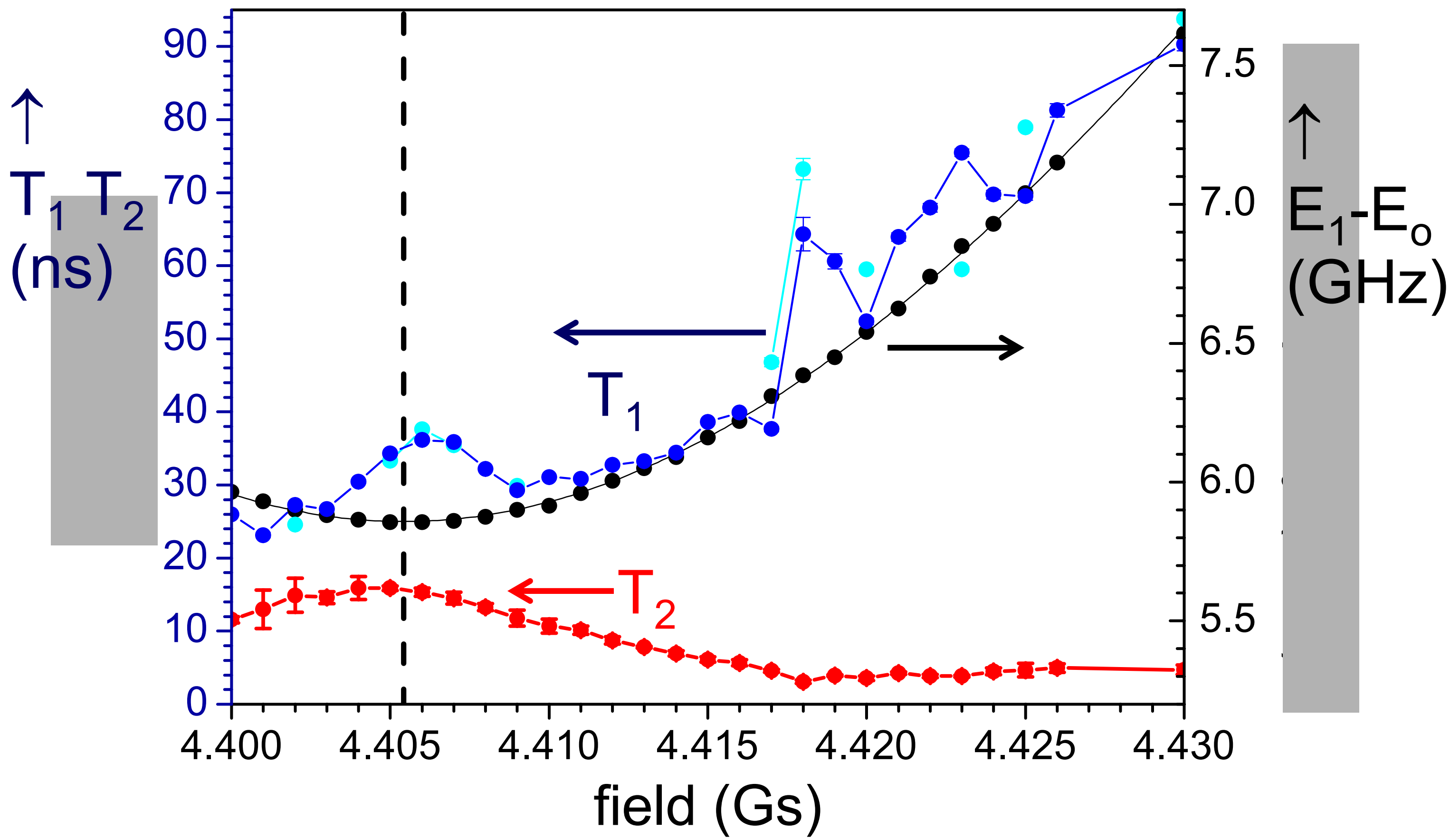

↑
T_1, T_2
(ns)
90
80
70
60
50
40
30
20
10
0
T_1
T_2
7.5
7.0
6.5
6.0
5.5
↑
E_1-E_o
(GHz)
4.400
4.405
4.410
4.415
4.420
4.425
4.430
field (Gs)

influence of bias current on T_1 and T_2

$$\frac{1}{T_2} = \frac{1}{2T_1} + \frac{1}{T_\varphi}$$

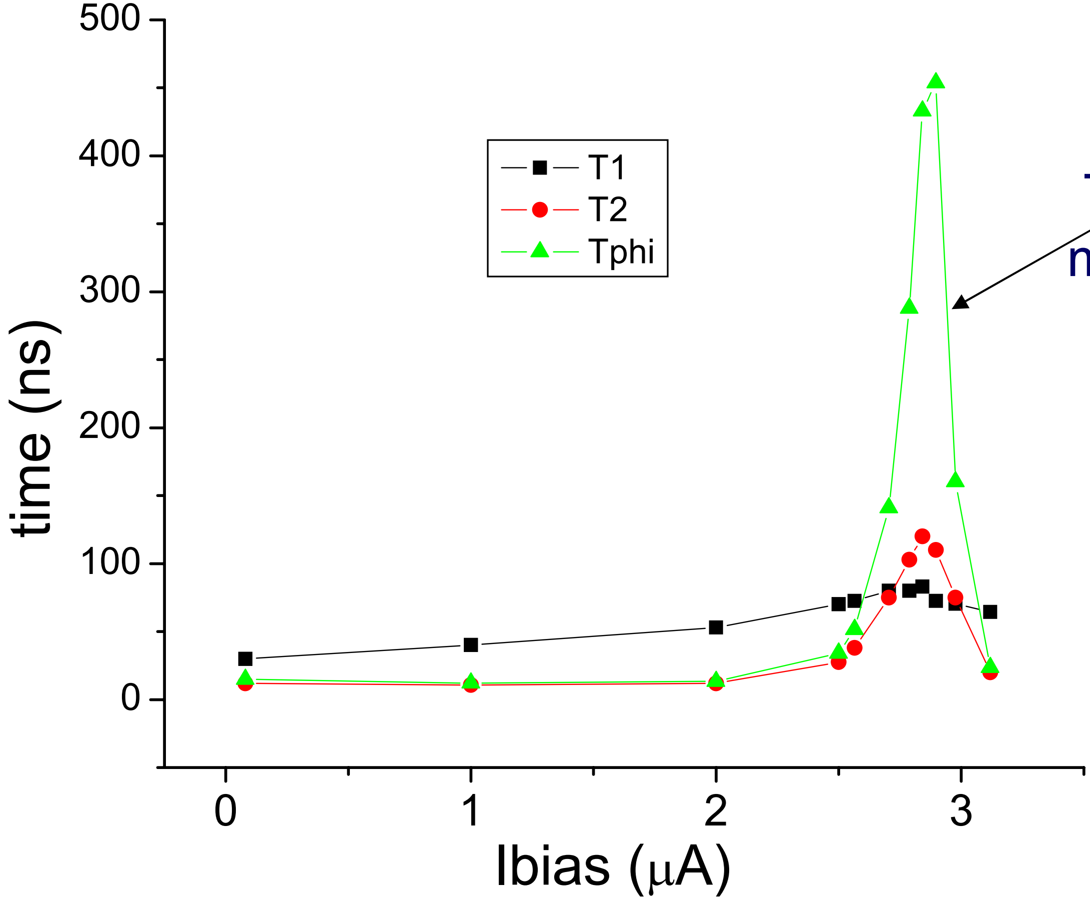

T_ϕ calculated from measured T_1 and T_2

black: T_1

red: T_2

Ramsey in presence of transport current

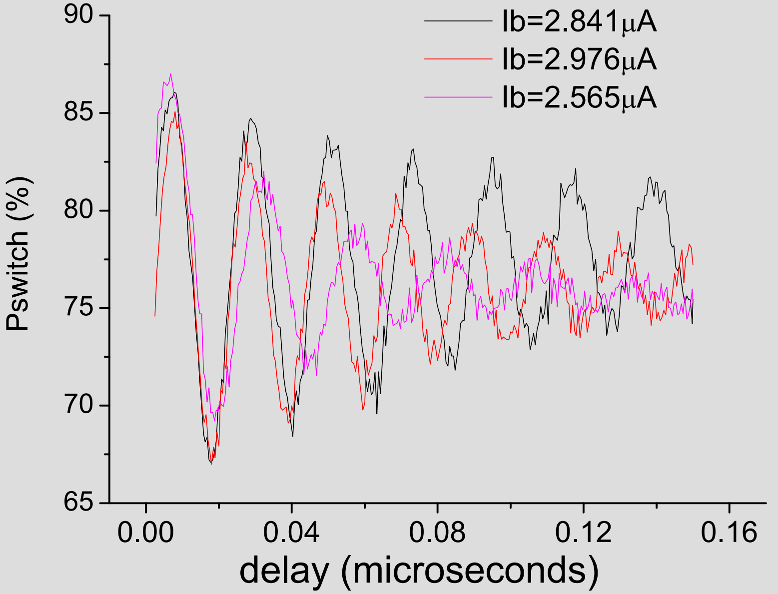

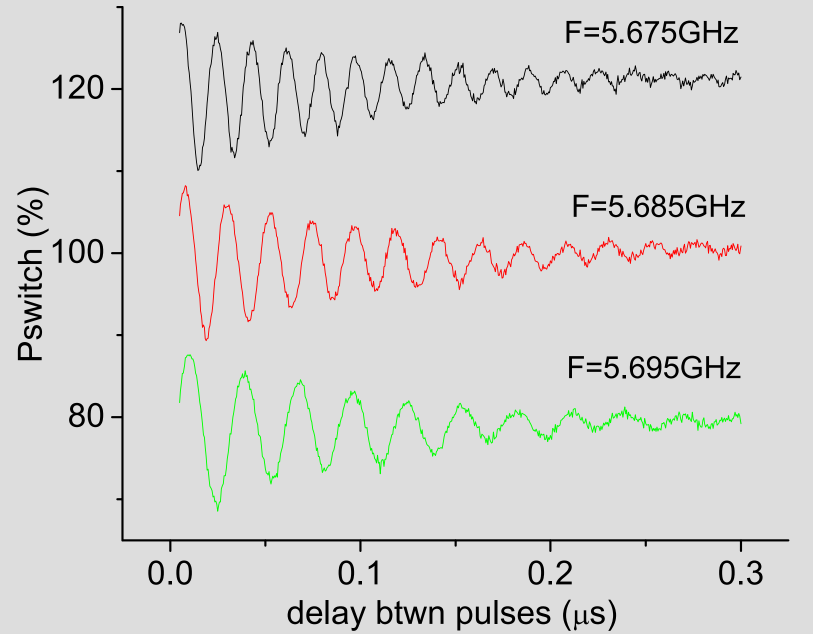

T_1=70ns
T_2=120 ns

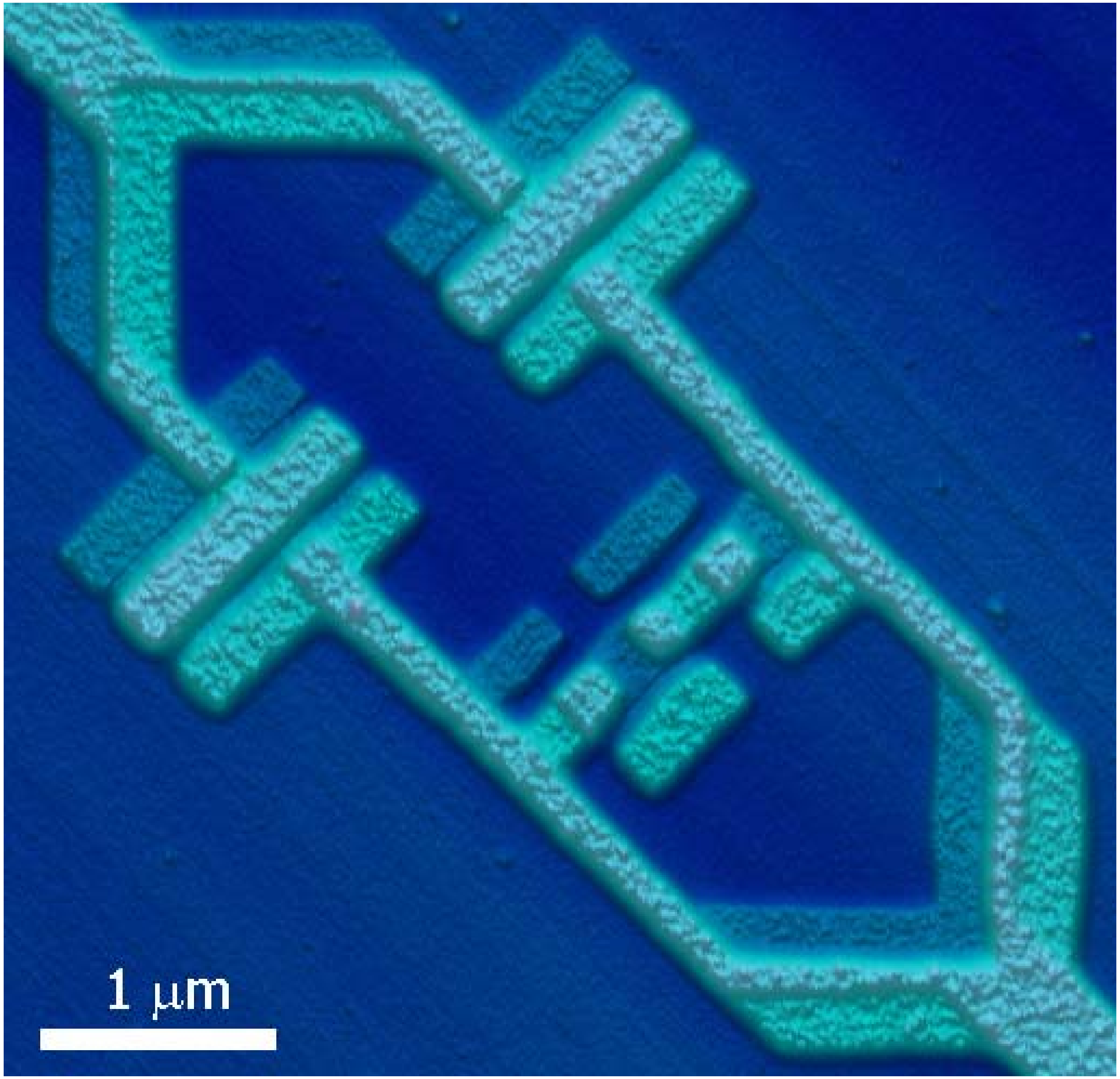

Patrice Bertet, Irinel Chiorescu

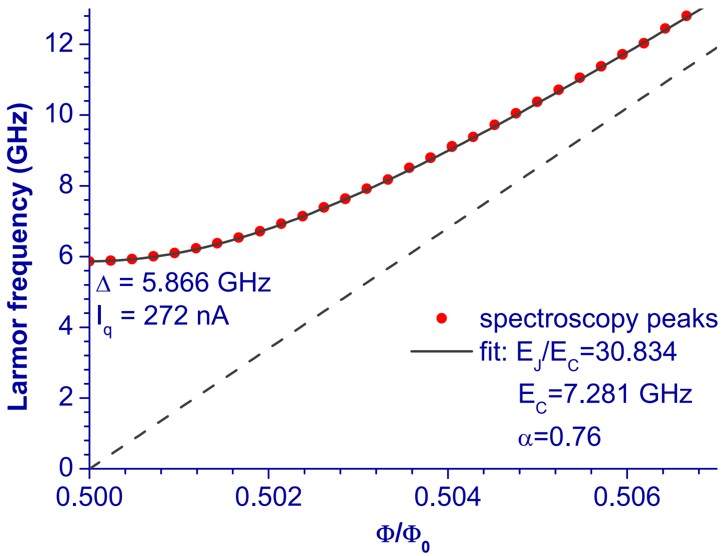

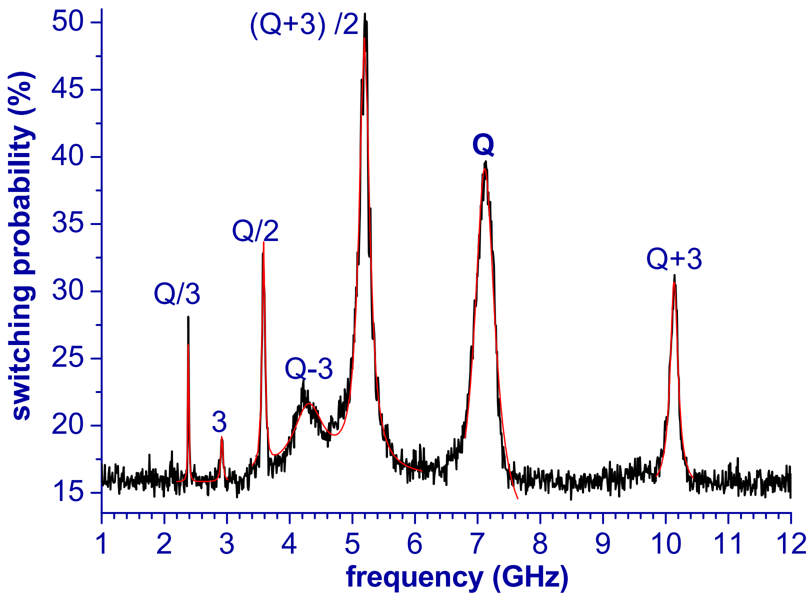

gap 5.866 GHz
persistent current 272 nA

spectroscopy peaks
Q: qubit 1,2,3 fotons
3: ω_p squid 2.91 GHz
Q±3: sidebands

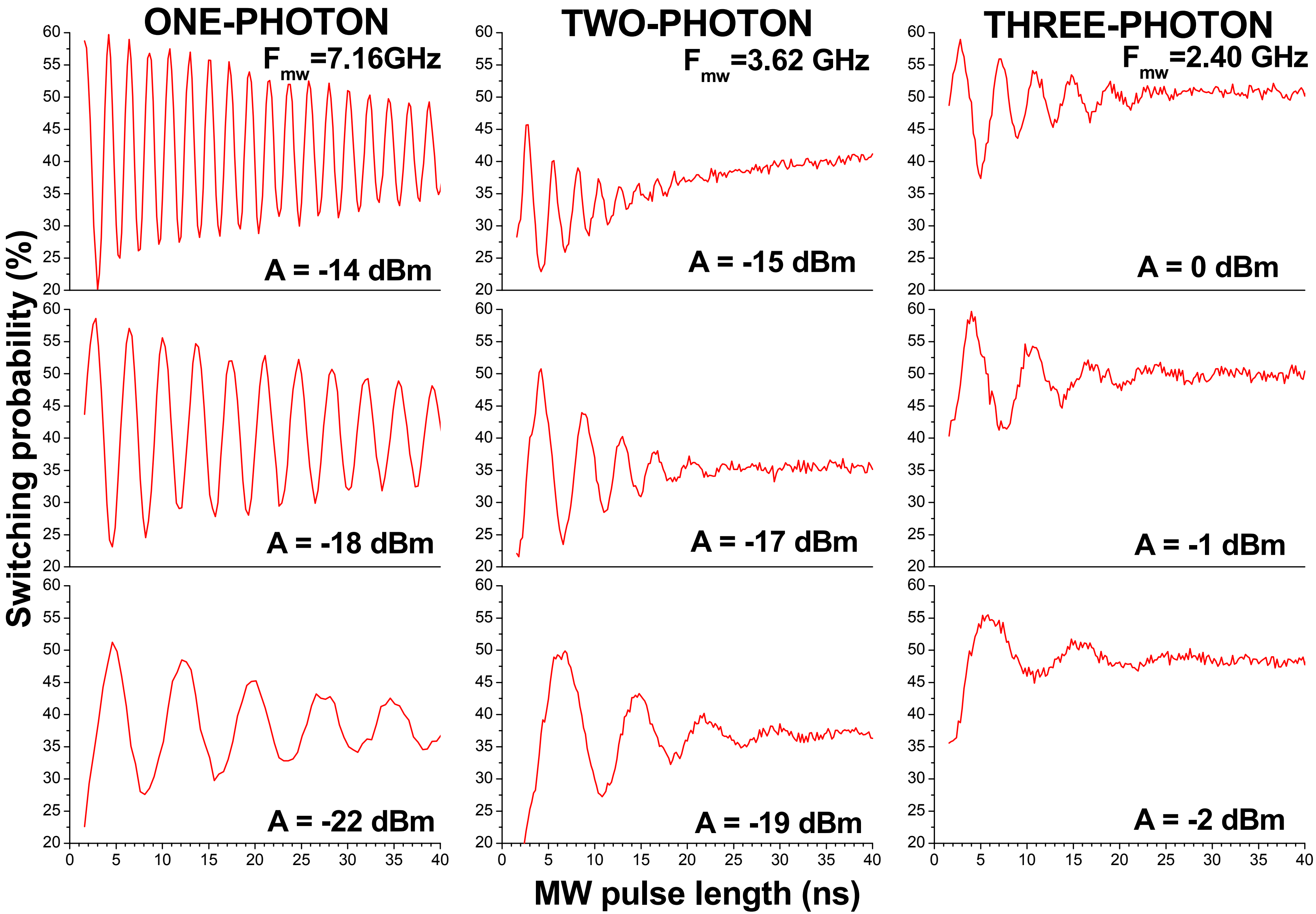
ONE-PHOTON
TWO-PHOTON
THREE-PHOTON
F_mw=7.16GHz
F_mw=3.62 GHz
F_mw=2.40 GHz
A = -14 dBm
A = -15 dBm
A = 0 dBm
A = -18 dBm
A = -17 dBm
A = -1 dBm
A = -22 dBm
A = -19 dBm
A = -2 dBm
Switching probability (%)
MW pulse length (ns)

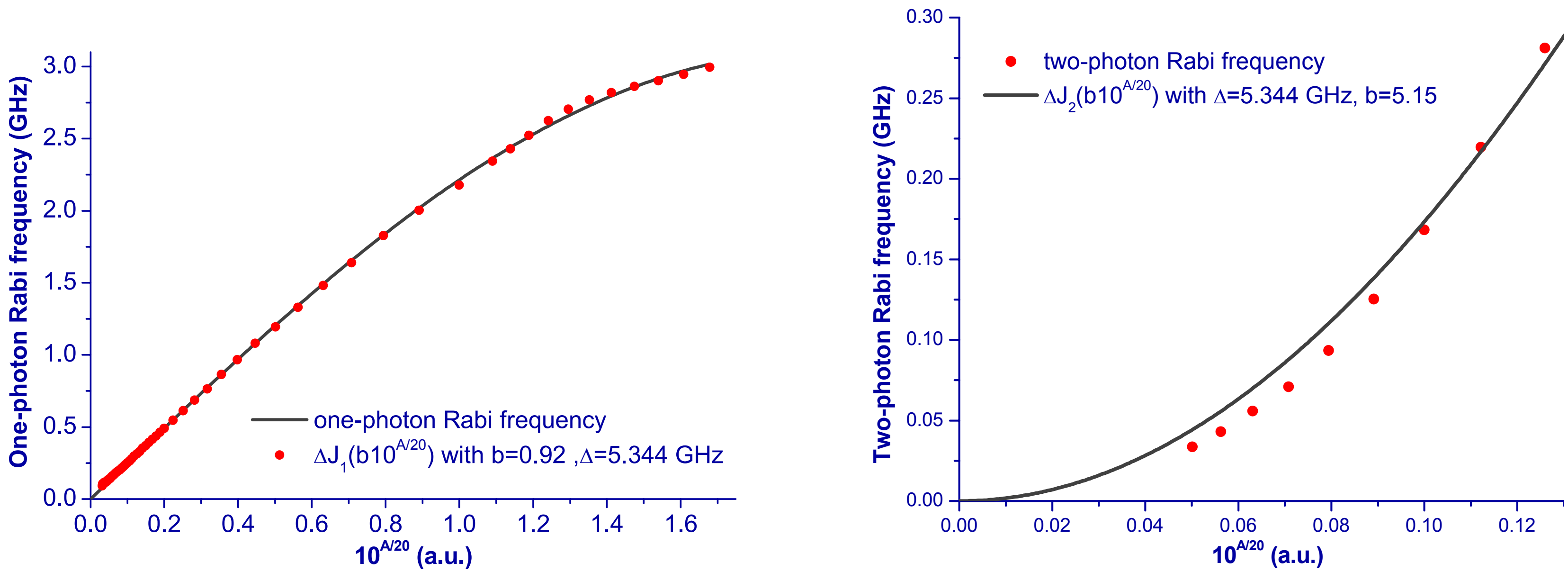

One-photon Rabi frequency (GHz)
3.0
2.5
2.0
1.5
1.0
0.5
0.0
0.0 0.2 0.4 0.6 0.8 1.0 1.2 1.4 1.6
10^A/20 (a.u.)
one-photon Rabi frequency
ΔJ1(b10^A/20) with b=0.92 ,Δ=5.344 GHz
Two-photon Rabi frequency (GHz)
0.30
0.25
0.20
0.15
0.10
0.05
0.00
0.00 0.02 0.04 0.06 0.08 0.10 0.12
10^A/20 (a.u.)
two-photon Rabi frequency
ΔJ2(b10^A/20) with Δ=5.344 GHz, b=5.15

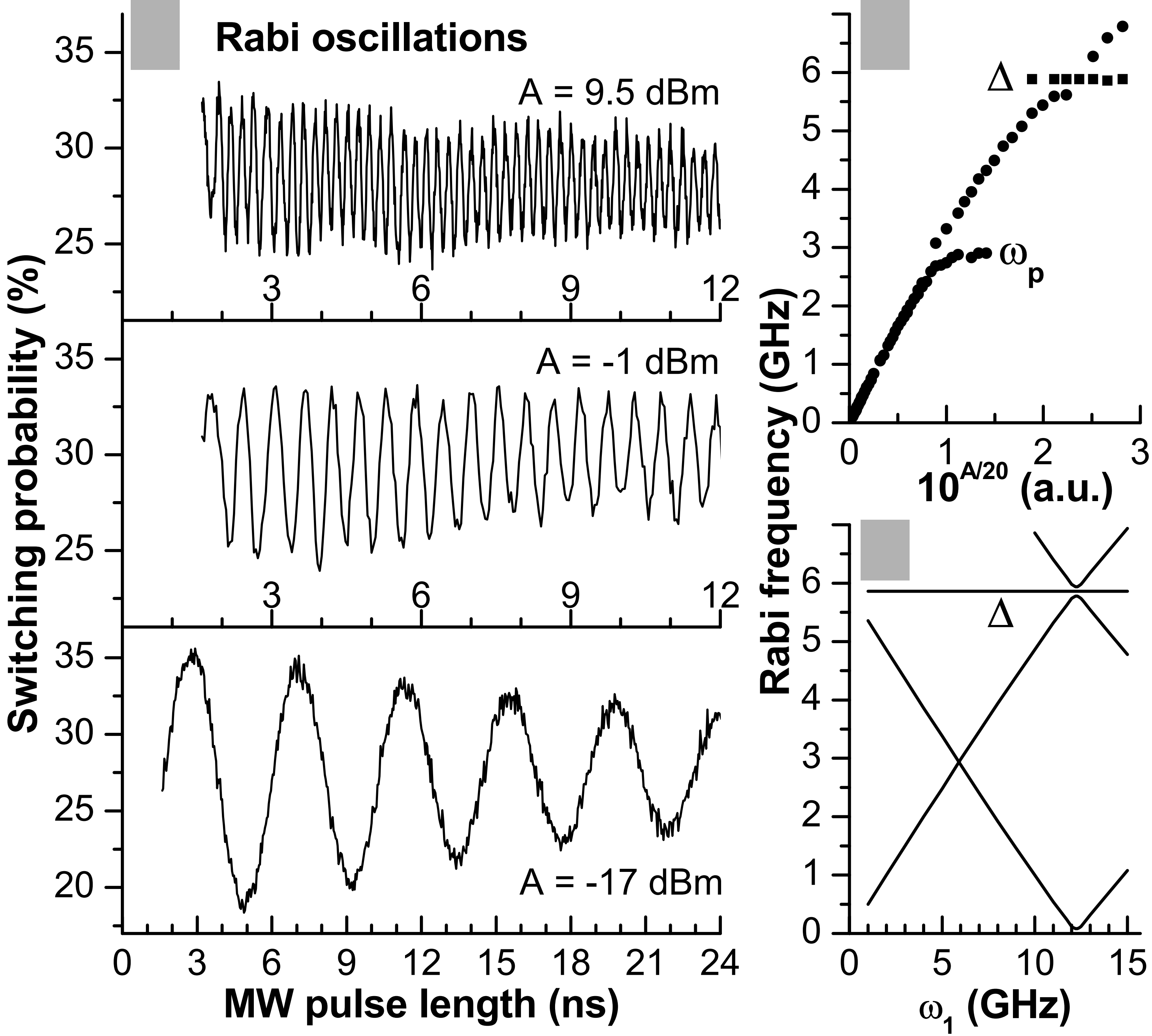

Rabi oscillations
A = 9.5 dBm
A = -1 dBm
A = -17 dBm
Switching probability (%)
MW pulse length (ns)
Rabi frequency (GHz)
Δ
ω_p
10^(A/20) (a.u.)
ω_1 (GHz)

flux qubit coupled to harmonic oscillator

harmonic oscillator: measurement SQUID shunted by large external capacitance; Q about 150

strong coupling accidental

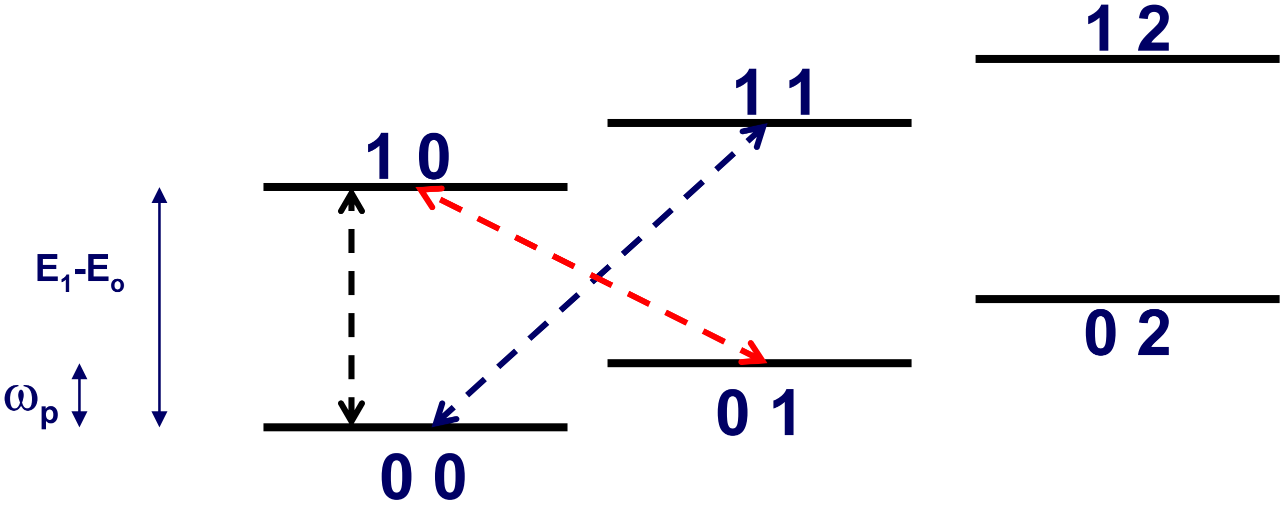

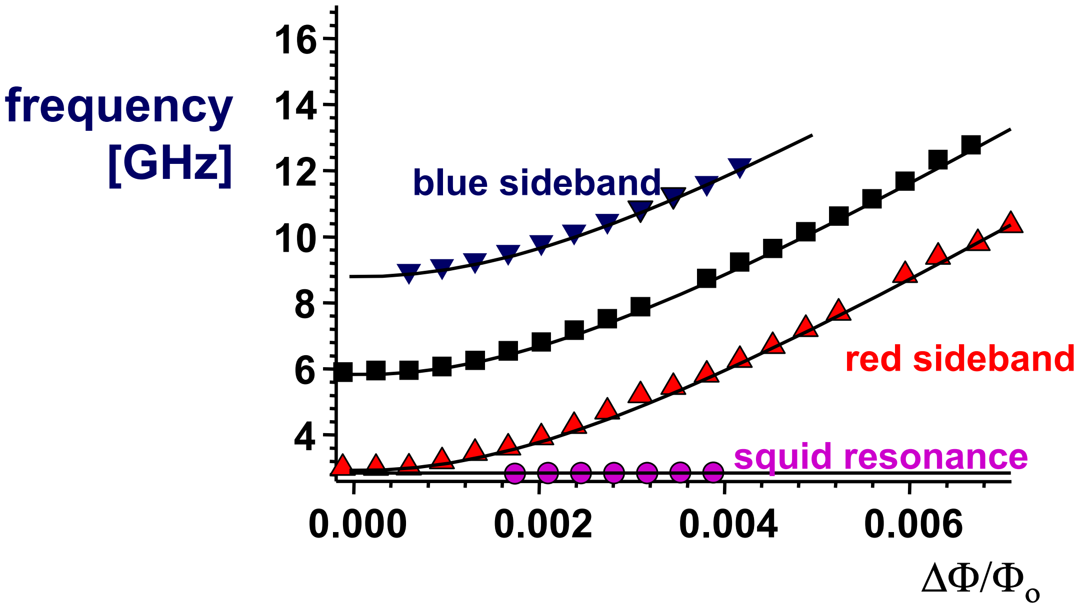
frequency
[GHz]
16
14
12
10
8
6
4
blue sideband
red sideband
squid resonance
0.000
0.002
0.004
0.006
ΔΦ/Φo

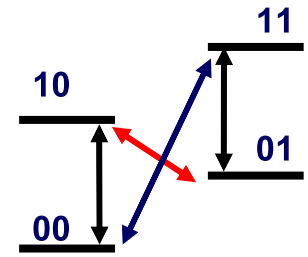
11
10
01
00

coherent oscillations of the coupled system

qubit Larmor frequency 7.16 GHz
plasma frequency : 2.91 GHz

coupled system at 10.15 GHz (blue sideband)

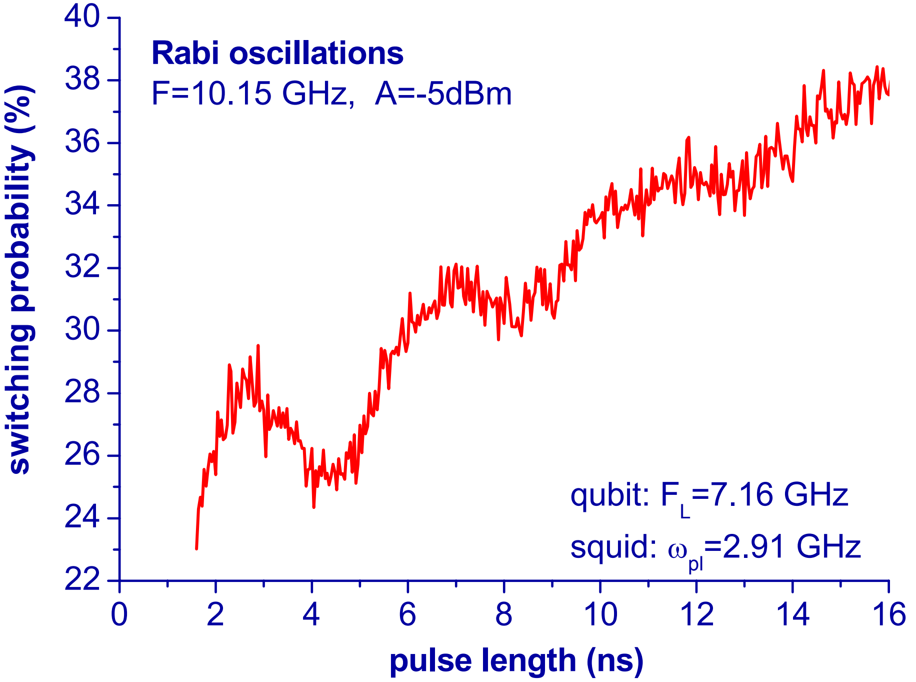

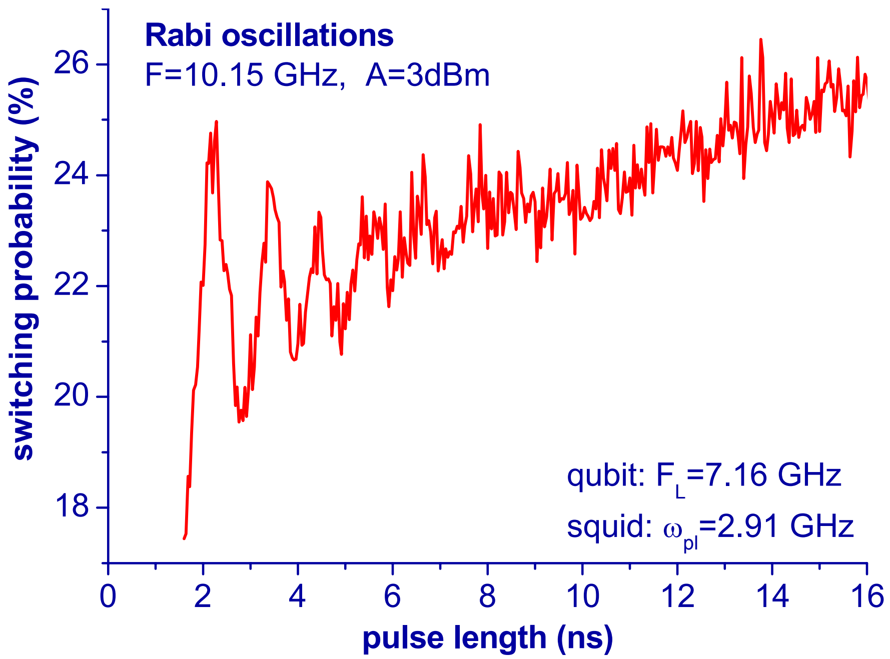

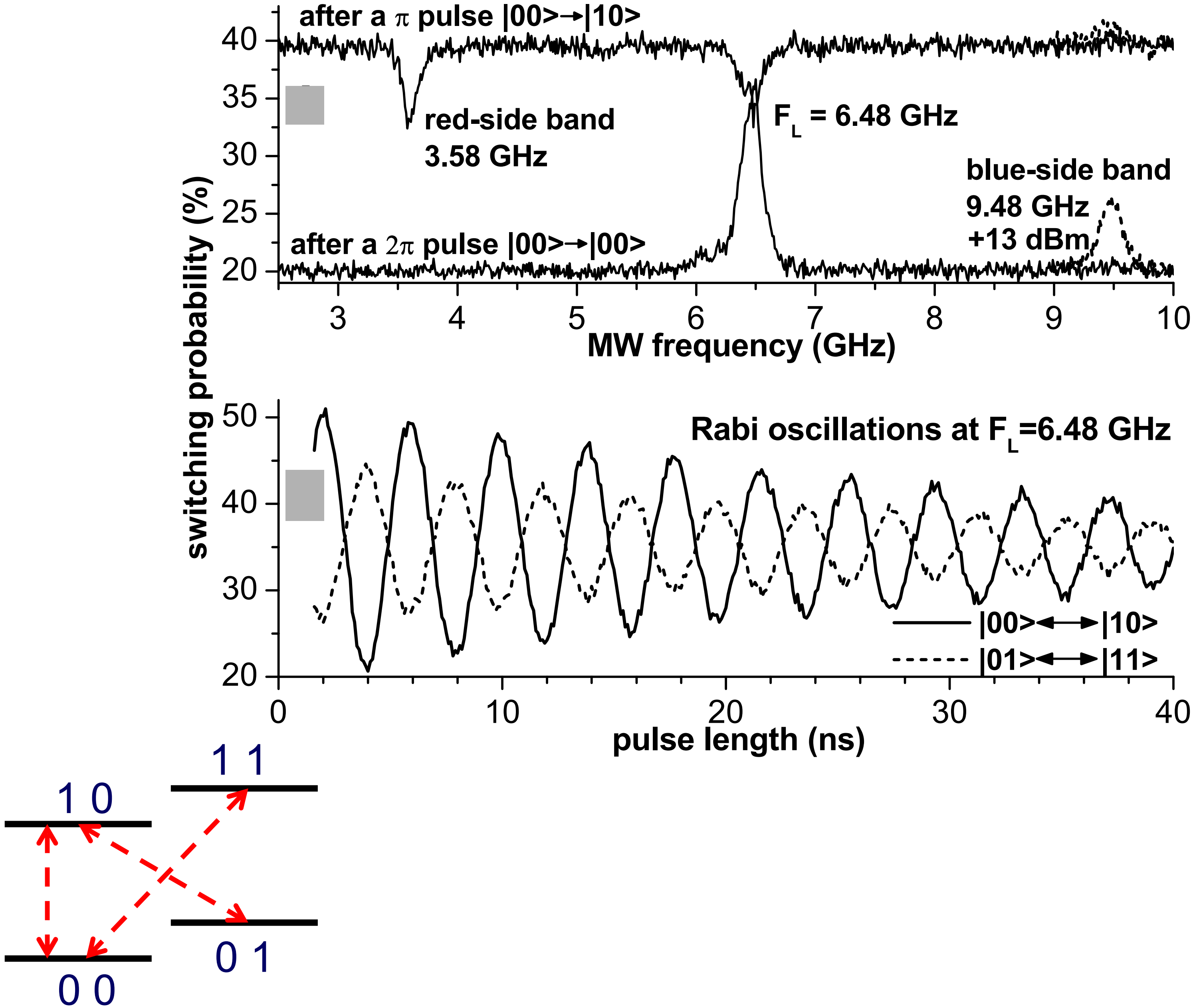
after a π pulse |00>→|10>
red-side band
3.58 GHz
F_L = 6.48 GHz
blue-side band
9.48 GHz
+13 dBm
after a 2π pulse |00>→|00>
switching probability (%)
MW frequency (GHz)
Rabi oscillations at F_L=6.48 GHz
|00>↔|10>
|01>↔|11>
pulse length (ns)
1 0
1 1
0 0
0 1

SQUID readout with qubit-dependent resonant pulse

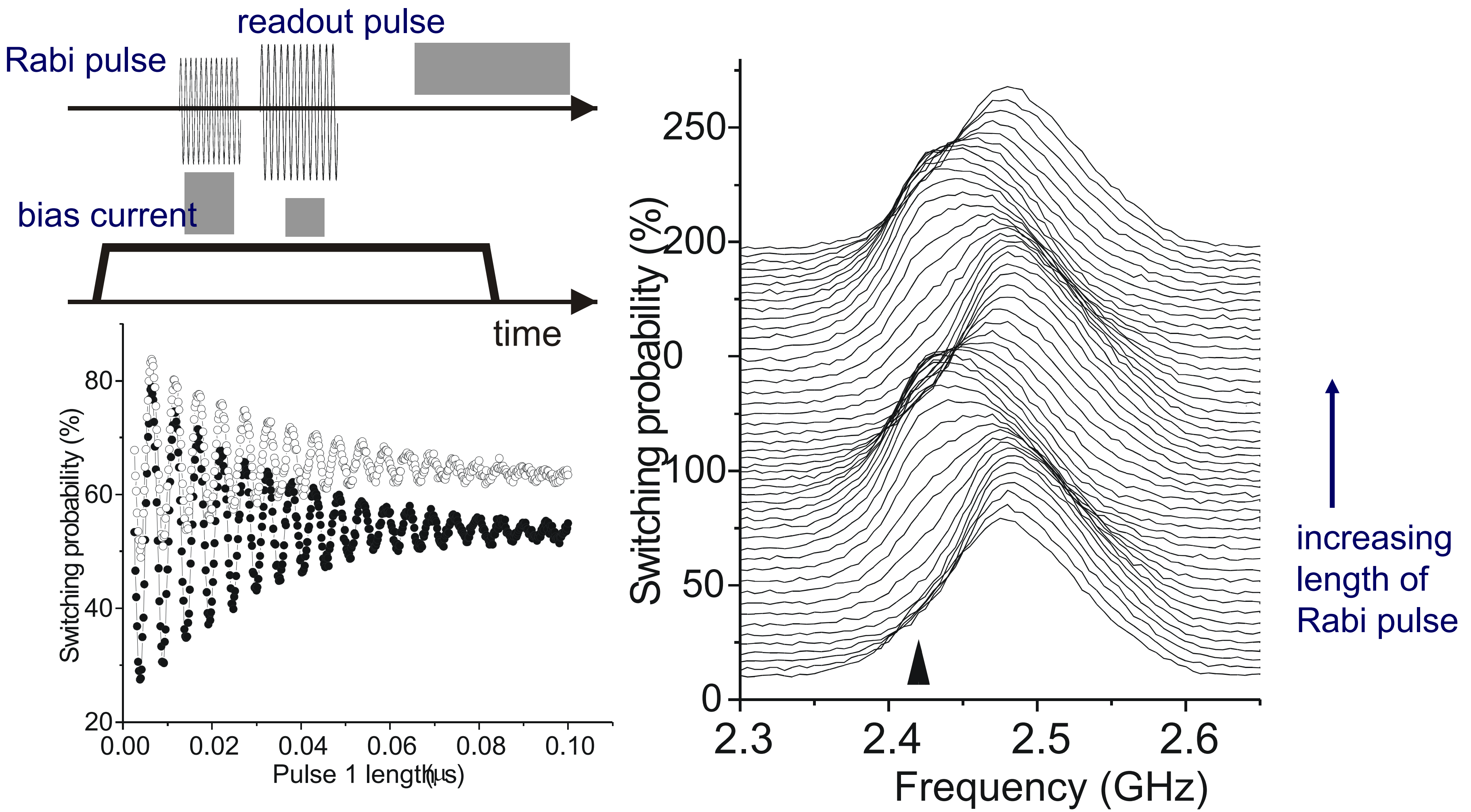

improved visibility

coupling of qubits

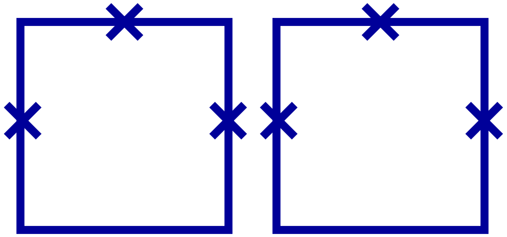

0.01 pH 4 MHz

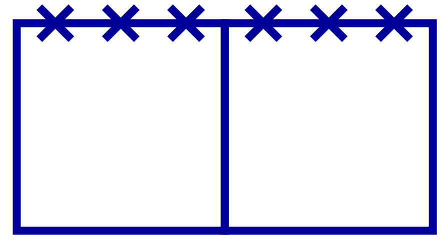

2 pH 0.8 GHz

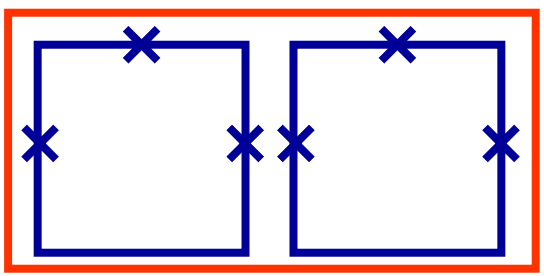

0.3 pH 0.1 GHz

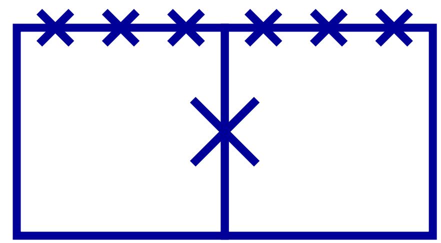

10 pH 4 GHz

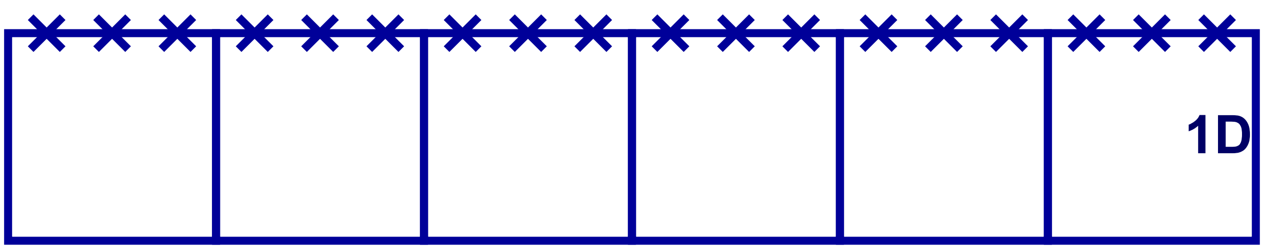

1D qubit chain

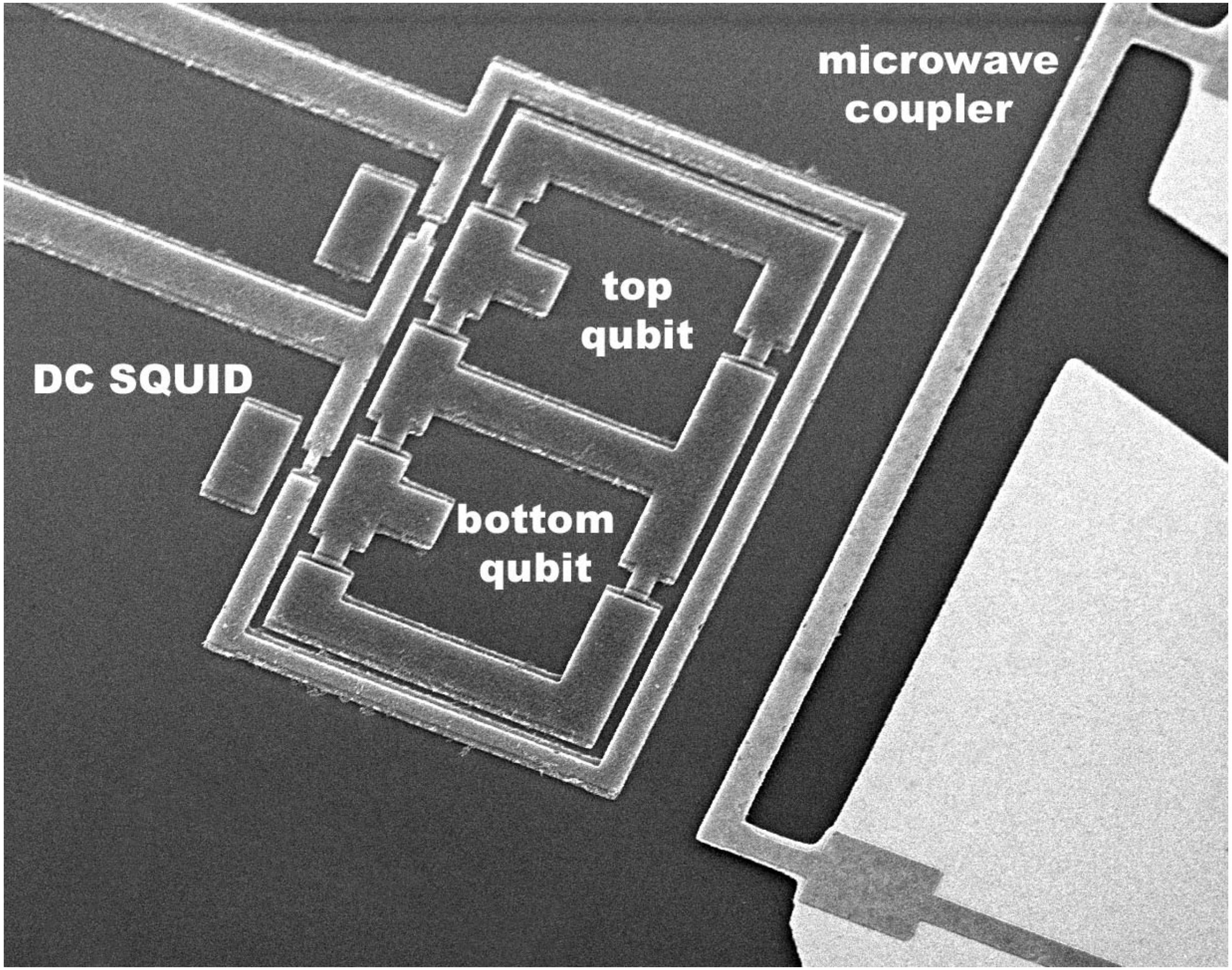

Hannes Majer
Floor Pauw
Alexander ter Haar

$$H = h_1\sigma_z^1 + t_1\sigma_x^1 + h_2\sigma_z^2 + t_2\sigma_x^2 + j\sigma_z^1\sigma_z^1$$

asymmetry in h: E_J and area (shift of f=0.5)

asymmetry t: E_J, junction ratio α

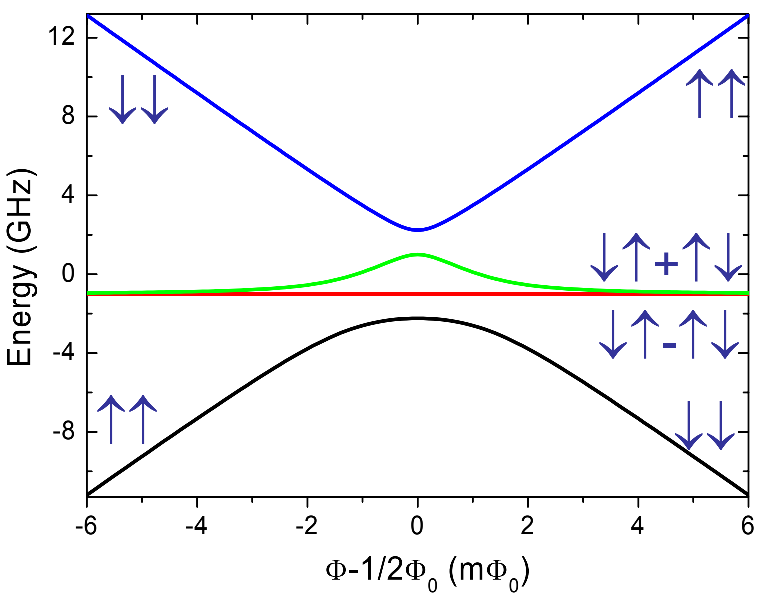

symmetric qubits

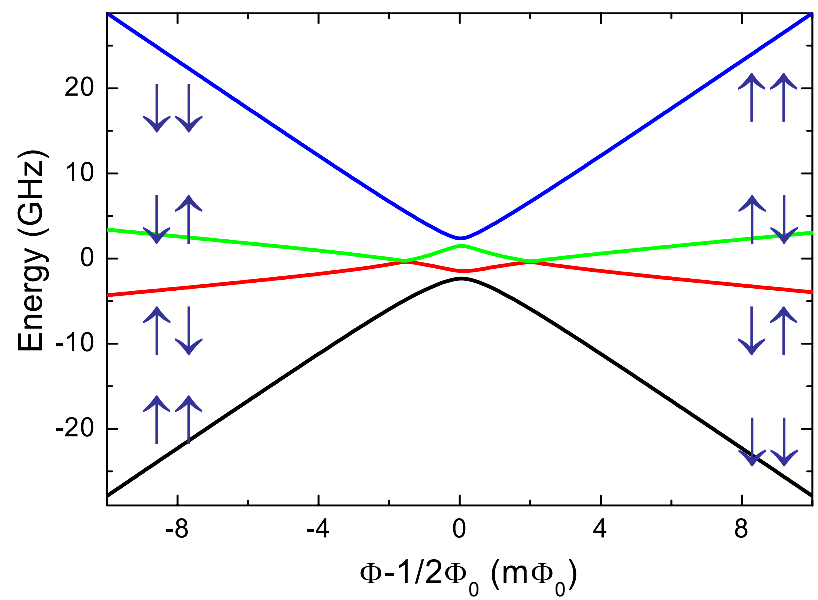

asymmetric qubits

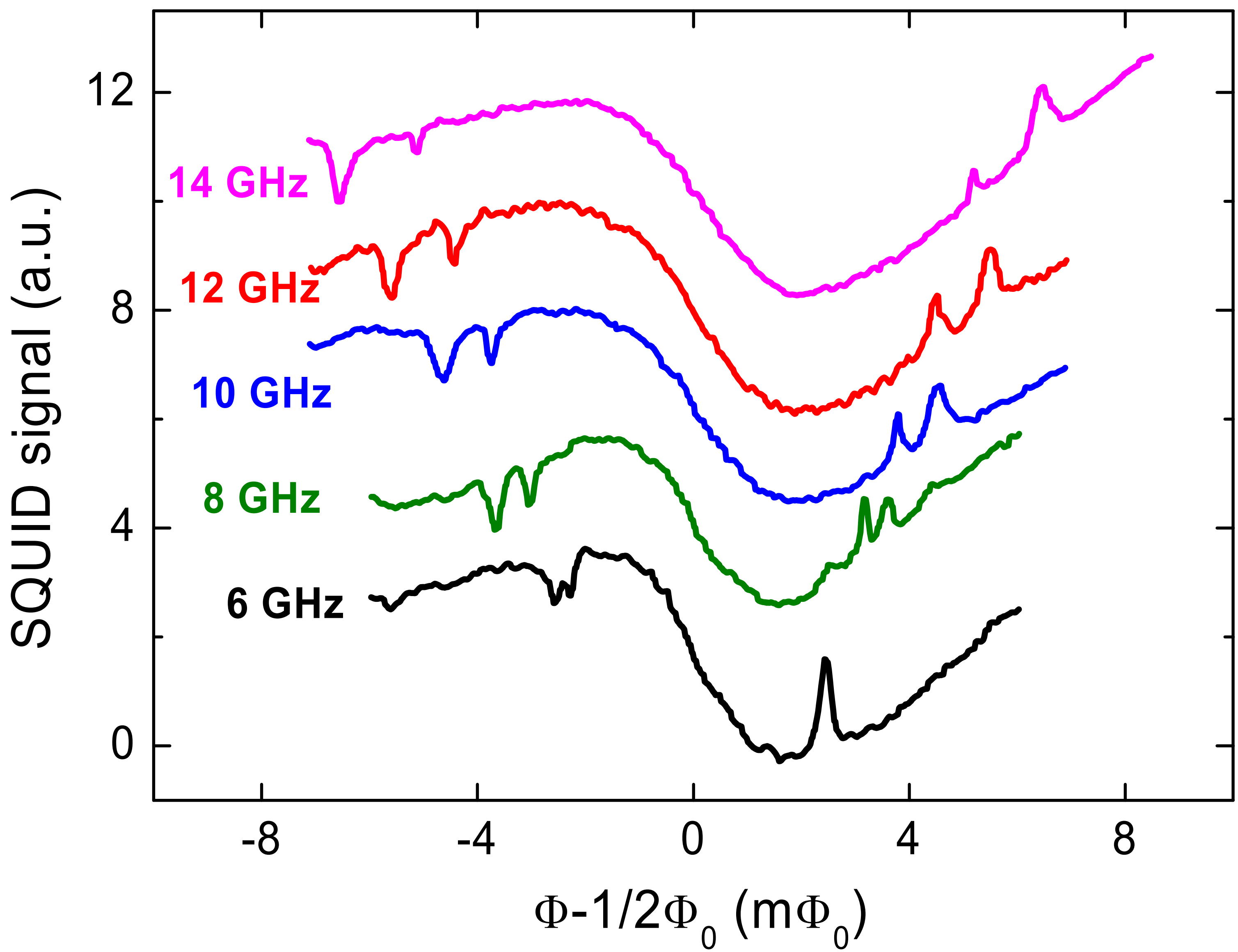

14 GHz
12 GHz
10 GHz
8 GHz
6 GHz
SQUID signal (a.u.)
12
8
4
0
-8
-4
0
4
8
Φ-1/2Φ0 (mΦ0)

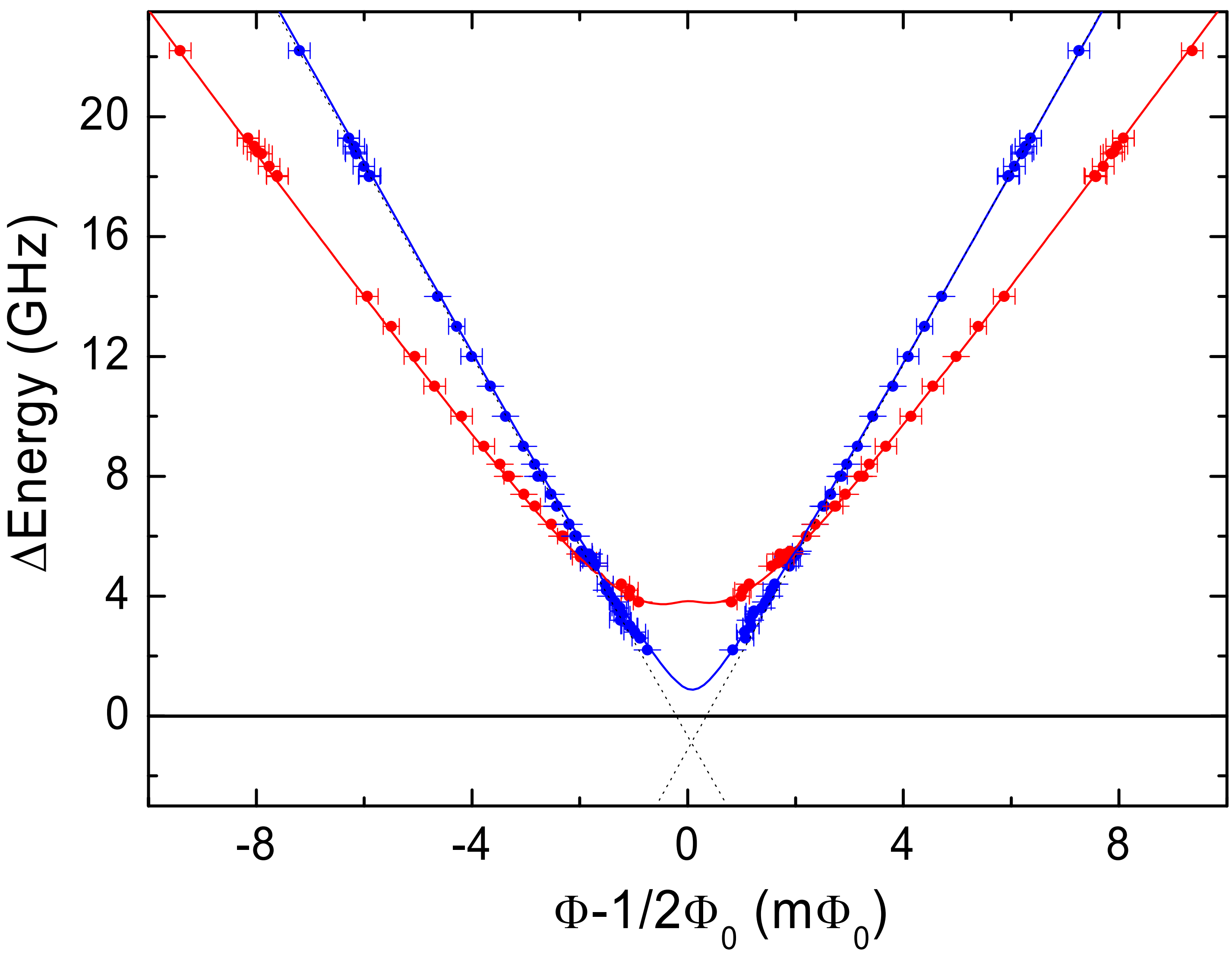

ΔEnergy (GHz)
20
16
12
8
4
0
-8
-4
0
4
8
Φ-1/2Φ0 (mΦ0)

results of fit

I_{p1} = 512 nA ± 6nA t_1 = 0.45 GHz ± 0.2 GHz

I_{p2} = 392nA ± 5nA t_2 = 1.9 GHz ± 0.1 GHz

sigma = -0.027% ± 0.004% (difference areas)

j = 0.50 GHz ± 0.03 GHz (coupling strength)

no transitions to 3rd excited state:

low transition probability

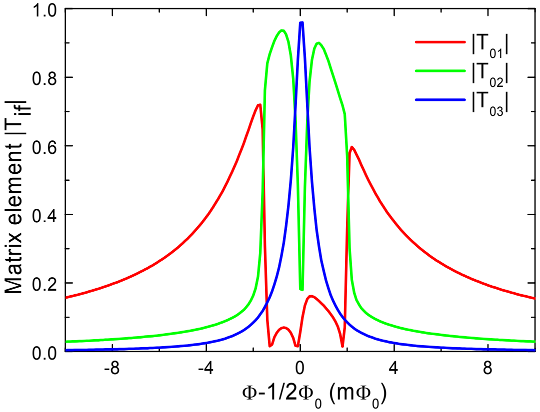

conclusions

- flux qubit behaves quantum mechanically

- coherent driving possible (to a certain extent)

- decoherence partly due to circuit, partly to defects

- coherent driving observed of 2-level system
  +harmonic oscillator

Delft flux qubits

Kees Harmans
Alexander ter Haar
Irinel Chiorescu
Adrian Lupascu
Floor Pauw
Patrice Bertet
Jelle Plantenga
Jonathan Eroms
Yasunobu Nakamura (NEC)
Kouichi Semba (NTT)

funding: FOM, EU
ARO, Kavli